UNIVERSITY OF NAIROBI

DEGRADATION AND ADSORPTION OF LAMBDA-CYHALOTHRIN ON ATHI RIVER AND COASTAL SOILS AND SEDIMENTS IN KENYA

BY:

SHERIFF SALIA S.

Reg. No: I56/81651/2015

This Thesis Submitted in Partial Fulfillment of the Requirements for Award of the Degree of Master of Science in Environmental Chemistry of the University of Nairobi

December 2017

DECLARATION

I declare that this thesis is my original work and has not been submitted elsewhere for research. Where other people's work or my own work has been used, this has properly been acknowledged and referenced in accordance to the University of Nairobi requirement.

Signature_____ Date_____

Sheriff Salia S.
I56/81651/2015
Department of Chemistry
School of Physical Sciences
University of Nairobi

This thesis is submitted for examination with my approval as research supervisor:

Signature_____ Date_____

Dr. Vincent Madadi
Department of Chemistry
University of Nairobi
P.O Box 30197-00100
Nairobi Kenya vmadadi@uonbi.ac.ke

DEDICATION

To my late Dad, Sekou Sheriff, whose moral and financial supports paved this path of academia; and to my mom, wife and kids whose love and courage have always strengthened me in time of difficulty and joy.

ACKNOWLEDGEMENT

Thanks to my supervisor, Dr. Vincent Madadi whose advice, insightful criticisms and patience aided the completion of this research innumerably; and to the late Prof. G.N. kamau. Special thanks go to the staffs of the Analytical Research Lab, the Department of Chemistry, Department of Physics, my sponsor, my fellow comrades and colleagues all of the University of Nairobi who supported me in one way or another toward the completion of this work. Your effort was greatly needed and deeply appreciated.

ABSTRACT

Lambda-Cyhalothrin is extensively used in agriculture, horticulture and public health management in Kenya. The pesticide is effective against many vegetable pests, rice and other related disease vectors. This study investigated adsorption of L-Cyhalothrin onto sediments of Athi River and degradation on Kwale and Athi River soils. Sample analysis was conducted using UV-Visible spectrophotometry and the results were analyzed by fitting data into isotherm models including Langmuir, Freundlich, Temkin, Dubinin-Radushvich and Scathard plot to understand the environmental impacts of this pesticide. The models presented different numerical values but the results demonstrated similar characteristics.
It stands out that Dubinin-Radushvich (D-R) with average R^2: 93.48, 93.75 and 89.8 fitted best in this experiment followed by Freudlich R^2: 78.28, 89.95 and 81.18 and Quasi-Langmuir R^2: 81.6, 87.45 and 70.53 for all samples from the upstream, midstream, and downstream of Athi River, respectively. The spontaneity of the adsorption process was also realized in ΔG values as predicted by Langmuir and Freundlich. In both models, the ΔG values for the midstream were negatives -9.781 KJ/Kmol and -2.720 KJ/Kmol for Langmuir and Freudlich, respectively. This showed complete spontaneous characteristics, whereas the ΔG value for upstream was positive (9.286 KJ/Kmol) for Langmuir and negative (-4.462.12 KJ/Kmol) for Freundlich. The downstream recorded a positive ΔG value (3.0968 KJ/Kmol) for Freudlich while Langmur was negative (-5.4415KJ/Kmol). Other important parameters in Freudlich, such as the number of adsorbed molecules, n and the apparent equilibrium constant K were determined. The average values were 1.04, 0.73, and 0.39 for n and 6.36, 2.89, and 0.54 for K, for upstream, midstream and downstream, respectively. Degradation of L-Cyhalothrin was faster in Kwale soil than Athi River soil with half-life between 4 to 5 weeks for Kwale soil was faster than Athi River soil. Adsorption modeling and degradation studies of pesticide residues are vital to environmentalist and policy makers in determining the application and disposal mechanisms for these pollutants.

TABLE OF CONTENTS

DECLARATION ..... **ii**
DEDICATION ..... **iii**
ACKNOWLEDGEMENT ..... **iv**
ABSTRACT ..... **v**
LIST OF TABLES ..... **ix**
LIST OF FIGURES ..... **x**
LIST OF ACRONYMS AND ABBREVIATIONS ..... **xii**

CHAPTER ONE **1**
INTRODUCTION **1**
1.1 Background of the Study 1
1.2 Environmental Fates 3
1.3 Statement of the Problem 4
1.4 Hypothesis of the Study 5
1.5 General Objective 5
1.6 Specific Objectives 5
1.7 Justification and Significance 6

CHAPTER TWO **7**
2. LITERATURE REVIEW **7**
2.1 Introduction 7
2.2 The Philippines Case 7
2.3 Nairobi case study 8
2.4 Adsorption Isotherms 9
2.4.1 Freudlich Isotherm 10
2.4.2 Langmuir Isotherm 14
2.4.3 Quasi Langmuir Isotherm 14
2.4.4 Temkin Isotherm Model 15
2.4.5 Dubinin-Radushkevich (D-R) Isotherm Model 15

CHAPTER THREE **17**
3. MATERIALS AND METHODS **17**
3.1 Area of Study and Collection of Samples 17
3.2 Apparatus and Instrumentation 18
3.3 Chemicals and Reagents 18
3.3.1 Determination of Available Soil/Sediments Nutrients 18
3.3.2 Determination of Organic Carbon 18
3.3.3 Total Nitrogen 18
3.3.4 Soil pH Determination 19
3.3.5 Trace elements Analysis 19
3.3.6 Cation Exchange Capacity at Neutral pH (Ca, Mg, K, and Na) 19
3.4 Preparation of Standards and Reagents 20
3.4.1 Preparation of Standard Reagents 20
3.5 Degradation Procedure 20

CHAPTER FOUR **21**
4. RESULTS AND DISCUSSIUON **21**
4.1 Sediments and Soil Characterizations 21
4.2 Absorption Profile of Lambda-Cyhalothrin 23
4.3 Effect of Sediment Mass 26
4.4 Effect Contact Time 27
4.4.1 Langmuir Isotherm Result 29
4.4.2 Quasi Langmuir Isotherm 32
4.4.3 Freudlich Isotherm Model 35
4.4.4 Temkin Isotherm Model 39
4.4.5 Dubinin-Radushkevich (D-R) Isotherm Model 42
4.4.6 Scatchard Plot Analysis 45
4.5 Degradation Studies 48

CHAPTER FIVE 51
5. CONCLUSION AND RECOMMENDATIONS 51
5.1 Conclusions 51
5.2 Recommendation 51
5.2.1 Recommendation from this Study 51
5.2.2 Recommendations for Further Work 52
REFERENCE 53

LIST OF TABLES

Table 4. 1: Athi River Sediment Profile used in the Adsorption Analysis. 21

Table 4. 2: Athi River and Kwale Soils used in degradation. 23

Table 4. 3: Data Summary for Adsorption Parameters. 28

Table 4. 4: Langmuir Isotherm Data. 30

Table 4. 5: Quasi-Langmuir Isotherm Data. 33

Table 4. 6: Freundlich Isotherm Data. 36

Table 4. 7: Temkin Isotherm Data. 39

Table 4. 8: Dubinin-Radushkevick Isotherm Data. 42

Table 4. 9: Scatchard Analysis Data. 45

Table 4. 10: Degradation Data for Athi River and Kwale Soils (ppm). 48

LIST OF FIGURES

Figure 1. 1: Structure of L-Cyhalothrin, (Rajendran & Phogat, 2013). 2

Figure 1. 2: Schematic Diagram for dissipation of pesticide in the Environment. 3

Figure 3. 1: Study Area. 17

Figure 4: 1: UV- Visible Spectra for L-Cyhalothrin (0-10 mg/L). 24

Figure 4: 2: UV-Visible Spectra of L-Cyhalothrin (0-100 mg/L). 24

Figure 4: 3: Plot of Absorbance against Concentration (0-10 ppm) of L- Cyhalothrin. 25

Figure 4: 4: Plot of Absorbance against Concentration (0-100) of L-Cyhalothrin. 25

Figure 4: 5: Plot of amount L-Cyhalothrin adsorbed (qe) vs. varied masses (g) of the sample. .. 26

Figure 4: 6: Plot of amount in solution (Ce) against varied masses (g) of the sample. 27

Figure 4: 7: Langmuir Isotherm model for Sample A. 31

Figure 4: 8: Langmuir Isotherm Model for Sample B. 31

Figure 4: 9: Langmuir Isotherm Model for Sample C. 32

Figure 4: 10: Quasi-Langmuir Isotherm Model for Sample A. 34

Figure 4: 11: Quasi-Langmuir Isotherm Model for Sample B. 34

Figure 4: 12: Quasi-Langmuir Isotherm Model for Sample C. 35

Figure 4: 13: Freundlich Isotherm Model for Sample A. 37

Figure 4: 14: Freudlich Isotherm Model for Sample B. 38

Figure 4: 15: Freudlich isotherm Model for Sample C. 38

Figure 4: 16: Temkin Isotherm Model for Sample A 40

Figure 4: 17: Temkin Isotherm Model for Sample B. 41

Figure 4: 18: Temkin Isotherm Model for Sample C. 41

Figure 4: 19: D-R Isotherm Model for Sample A. 43

Figure 4: 20: D-R Isotherm Model for B. 43

Figure 4: 21: D-R Isotherm Model for Sample C. 44

Figure 4: 22: Scatchplot for Sample A. 46

Figure 4: 23: Scatchard Plot for Sample B. 47

Figure 4: 24: Scatchard Plot for Sample C. 47

Figure 4: 25: Degradation of L-Cyhalothrin in Athi River and Kwale Soils. 49

Figure 4: 26: Rate Degradation of L-Cyhalothrin in Athi River and Kwale Soils. 49

LIST OF ACRONYMS AND ABBREVIATIONS

BIS	Bureau of India Standards
C_{ad}	pesticide concentration adsorbed
CDPR	California Department of Pesticide Regulation
EPA	Environmental Protection Agency, USA
FAAS	Atomic Absorption spectrometer
G	Gibbs free energy
KALRO	Kenya Agricultural and Livestock Research Organization
KEPHIS	Kenya Plant Health Inspectorate Sservices
K_F	Freundlich Constant
n	measure of non-linearity constant in Isotherm/number of active sites
NPIC	National Pesticides Information Center
PCB	Polychlorinated Biphenyls
USEPA	United States of America Environmental Protection Agency
USA	United States of America
UV-Vis	Ultra Violet and Visible Light
WHO	World Health Organization, UN

CHAPTER ONE

INTRODUCTION

1.1 Background of the Study

The use of pesticides (insecticides, herbicides, fungicides, rodenticides and acaricides) can be dated before 16th century when chemicals such as arsenic sulphide, Paris green (Copper acetoarsenite) were used to control Malaria-transmissions, though the use of synthetic organic pesticides began around 1940 (De, 2010). Lambda-Cyhalothrin is a synthetic insecticide that has similar biochemical effects to that of natural pyrethrin pesticide (He *et al*., 2008) . It is the active ingredient in locally used insecticides with trade names such as Karate, Warrior, and Icon that are commonly applied to control insects and/or pests in public health emergency, agricultural/horticultural farming, and in homes (CDPR, 2006). It is effective against many crop and disease vector insects including potatoes, cereals, cotton, vegetables, mosquitoes, cockroaches, flies and ticks (He *et al*., 2008). Lambda-Cyhalothrin also kills many insects in their earlier forms of life. The pesticide works better against the eggs and larvae of insects (Lawler *et al,* 2007). L-Cyhalothrin is synthesized from two stereoisomers of cyhalothrin combined in a 1:1 ratio; (S)-α-cyano-3-phenoxybenzyl-(z)-(1R,3R)-3-(2-chloro-3,3,3-trifluoroprop-1-enyl)-2,2-dimethylcyclopropanecarboxylate and (R)-α-cyano-3-phenoxybenzyl-(z)-(1S,3S)-3-(2-chloro-3-3,3-trifluoropropp-1-enyl)-2,2-dimethylcyclopropane carboxylate (BIS, 1997). Figure 1.1 shows the Structural formula of Lambda-Cyhalothrin:

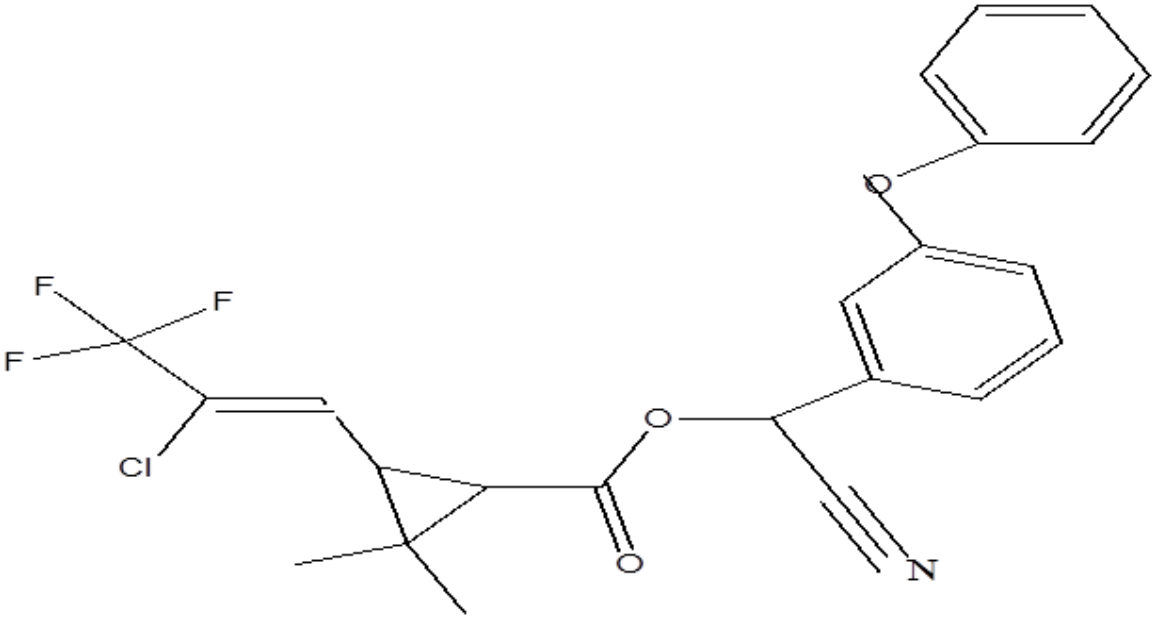

Figure 1. 1: Structure of L-Cyhalothrin, (Rajendran & Phogat, 2013).

L-Cyhalothrin appears white-like solid substance at standard room temperature and yellow in solution with low volatility. It has molecular weight of 449.9g/mol and molecular formula of $C_{23}H_{19}ClF_3NO_3$ (BIS, 1997). Lambda-Cyhalothrin and other pyrethroid pesticides used in livestock and crop farming due to their effective ability to prevent and cure crop diseases as well as to control vector-pests which has led to improved food security and livelihood in many developing countries. However, uncontrolled excessive use of the pesticides is hazardous to human life as well as the environment (FAO/WHO, 2012). Acute (short-term) human exposure leads to skin contact: (moderately; irritation, burning or prolong skin contact can cause allergic reaction), Ingestion: (vomiting or pulmonary injury, even death), and inhalation causes: (irritation to respiratory tract, headache, anesthesia, unconsciousness, nervous system effects or death) (Sharda, 2013). It is very toxic particularly to various species of fish and other aquatic organisms (He *et al*., 2008).

1.2 Environmental Fates

Lambda-Cyhalothrin is applied against insects due to its effective chemical action to pests and the rapid disappearance upon application in the environment (Serono *et al.*, 2016). Studies have proven that approximately 2-5% of applied pesticides go to targeted organisms and subsequently the rest end up contaminating the environment (Garcia *et al.*, 2011). Pesticide substrates in the environment undergo several chemical processes including oxidation, absorption, degradation, halogenation, transfer and other microbial actions (De, 2010). The transfer of pesticide residues away from the targeted sites through volatilization, spray drift, agricultural runoff, leaching, or crop removal is a major determining factor in assessing the overall environmental impacts of pesticides (Serono *et al*., 2016) as shown in Figure 1.2:

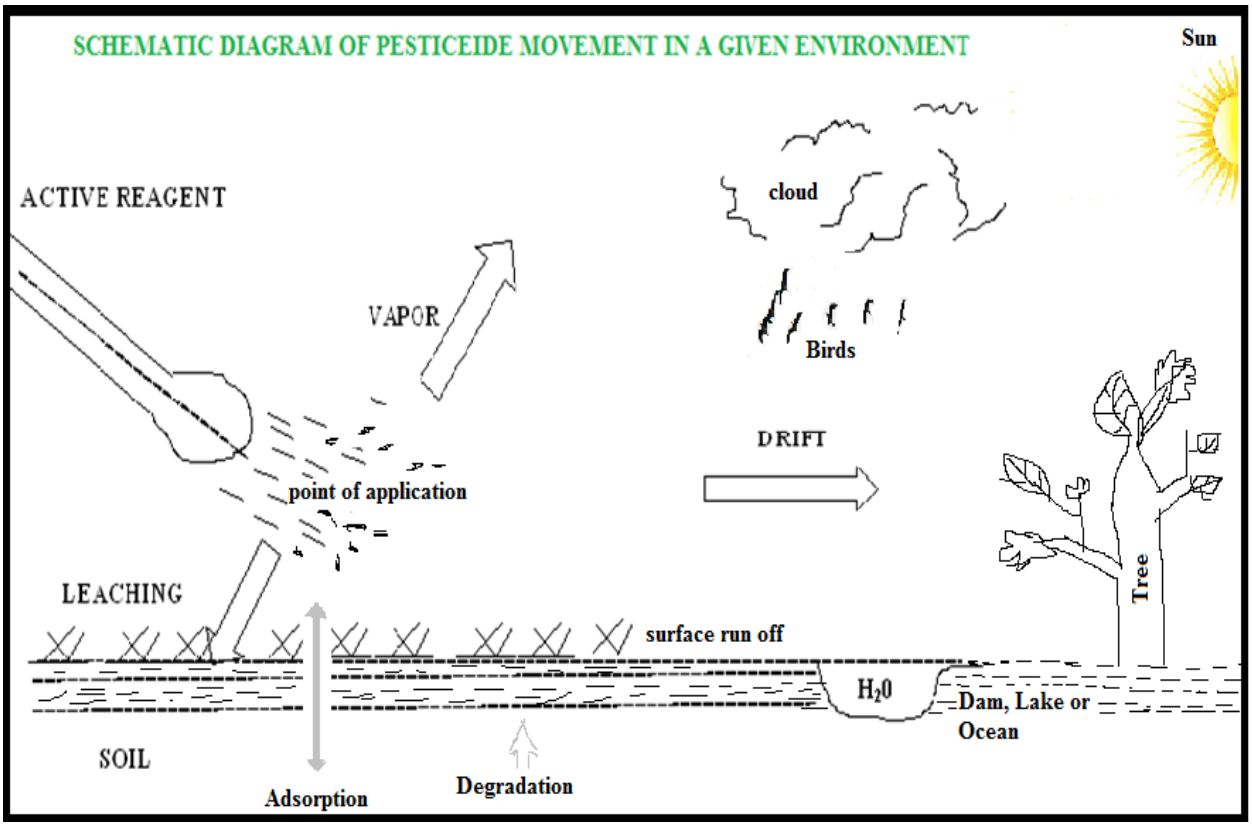

Figure 1. 2: Schematic Diagram for dissipation of pesticide in the Environment.

Figure 1.2 shows some typical transfer mechanisms of a pesticide in the environment after its application. Many processes take place after pesticide application, for example, runoff move the herbicide away from target place leading to chemical wastage and pest control (Markle *et al.*, 2014). There is also possibility of it causing damages to other non-target plants and insects, polluting soil, and wetlands, and consequently increasing biodiversity loss (Mbui, 2014).

In addition, the binding of pesticides onto soil and sediment particles vary with pesticide types, soil pH, soil moisture and organic carbon contents as well as soil textures (Jong and Byoung, 1997). The ability of pesticides to stay in the environment for a period of time allows them to affect aquatic ecosystems mostly non-target organisms such as crustaceans (McLaughlin, 2009); (Lewis *et al*., 2009). This effect is possibly manifested through the reduction in predator's fish populations notably those feeding on crustaceans or through direct consumption or contact from the environment. It may also be evidence from fish consuming human health, because laboratory studies show that a number of pesticides have potentials to accumulate in many different fish species (WHO, 1991).

1.3 Statement of the Problem

Pesticides are essential in public health protection and agricultural food production through crops and livestock protection against pests and disease vectors eradication of diseases such malaria and typhoid (De, 2010). Consequently, this has led to increased food production as well as improved livelihood in many developing countries. However, poor handling and excessive use of pesticides is hazardous to the general environment due to contamination/pollution challenges of surface and underground water, aquatic organisms, plants (food) and animals intoxication, including human and other biodiversity species (Manigandan *et al*., 2013). L-Cyhalothrin has been detected in pomegranate fruit residues and some other vegetables (Hem *et al*., 2010).

Ingestion and/or Inhalation of Lambda-Cyhalothrin can cause severe pulmonary injury, anesthesia, drowsiness, or may aggravate existing chronic respiratory and skin diseases (Sharda, 2013). Gastrointestinal and neurological problems, as well as problems in the endocrine and hormonal systems have been linked to pesticides in general (CDPR, 2011).

Therefore, there is need to study the presence of these pesticides in the environment, as well as their adsorption and degradation phenomenon, which control fate and transport of these compounds.

1.4 Hypothesis of the Study

Null hypothesis: Lambda-Cyhalothrin does not dissipate far from the point of application in Athi River and Kwale soils due to its high affinity on soil organic matter.

Alternative hypothesis: L-Cyhalothrin does not move far from the point of application in Athi River and kwale from soils since it is not strongly adsorbed to these soils.

1.5 General Objective

The overall objective is to investigate the adsorption and degradation of Lambda-Cyhalothrin onto Kwale soil and the Athi River soil and sediments.

1.6 Specific Objectives

i. To determine the adsorption capacity of Lambda-Cyhalothrin on sediments from the Upper, Middle and Down streams along the Athi River.
ii. To investigate the degradation of L-Cyhalothrin in Athi River and Kwale soils.
iii. To study the thermodynamic properties of L-Cyhalothrin in Athi River soils and sediments and Kwale soils using adsorption isotherm models such as Langmuir, freudlich, Temkin and Dubinin.

1.7 Justification and Significance

Athi River passes through the cement manufacturing industries and Athi River town as it flows downwards to the Indian Ocean. Occurrence of L-Cyhalothrin in sewage, industrial wastes and underground water has been acknowledged in several World Health Organization (WHO) reports (WHO, 2013). The exposure of farmers and consumption of foods contaminated with pesticide residues are among the key concerns to the general public. Therefore, there is need to study the contamination levels of the pesticide (L-Cyhalothrin) in soils and sediments. Athi River is a major source of water and irrigation for the human population and farmers along its bank. These farmers and other users are potentially exposed to the pesticide and other chemical wastes associated with the river.

CHAPTER TWO

2. LITERATURE REVIEW

2.1 Introduction

Previous studies have shown that the presence of pesticides including Lambda-Cyhalothrin in soils and sediments depend on the chemical compositions, absorption/adsorption properties and the concentrations of the pesticide (Espino, 2008). A research on pesticides in organic farms using similar procedure adsorption of chlorpyrifos and photo-degradation of pesticide residues was carried out in Limuru, Kenya by Mbui and co-workers (2014) alluded to the same argument.

2.2 The Philippines Case

A contemporary study carried out in the Philippines to determine environmental mode of transportation and fate of four pesticide residues including Lambda-Cyhalothrin in soil, water and air showed that 95%-98% of the applied pesticides migrated from treated areas to nearby soil, air and water (Arias *et al.*, 2008). It was recorded that lambda-Cyhalothrin was found from 2 meters to 20 meters away from target fields in air in varying concentrations of potential hazards (Serono *et al*., 2016). In water, the model prediction showed that L-Cyhalothrin could travel 200 meters away in 12 years (Wauchope *et al*., 1992). This proves the strong affinity of L-Cyhalothrin to soil and sediments as compared to other pesticides used in the research (Serono *et al*., 2016). Degradation of pesticides can be enhanced by increasing temperature and sunlight (Babu *et al.*, 2011).

The model calculation also showed that about half of the initial concentration of L-Cyhalothrin sample degraded in eight and half years, from 2007-2015 (NPIC, 2015). Under regular application of Lambda-cyhalothrin, the soil half-life was found to be about 30 days (NPIC,

2001). This indicates that L-Cyhalothrin has a potential of accumulating in animals and other biodiversity species (Serono *et al*., 2016).

2.3 Nairobi Case Study

In Nairobi, about 4 million residents including foreign visitors eat vegetables on regular basis. The city population is projected to rise to about 2.5 million more in a decade (GoK, 2003). This exponential population increase poses huge demand for food under the constraining condition of land scarcity (UNICEF *et al*., 2005).

There are about 3,000 farmers within Nairobi and its suburbs practicing horticultural/agricultural activities (Hide *et al*., 2001). Fifty percent (50%) of these farmers use poor quality water, untreated manure and do not follow standard application procedures for pesticides and other agrochemicals (Kang' ethe *et al.*, 2007). According to a research by the University of Nairobi and Sweden, kales (vegetables) from Nairobi City contain full spectrum of disease causing organisms (Lagerkvist *et al*., 2013). Vegetables are often grown on small plots along the sewer lines and polluted rivers due to the increasing cost of lands for commercial and domestic purposes and accessibility to irrigation water (Kilelu, 2014). Farmers regularly use untreated industrial wastewater with bounty of effluents for vegetables farming. For example Nairobi River, Ngong River and Athi River water is used by city residents for urban farming, domestic and even industrial activities (Mbui, 2014). At the Dandora Wastewater Treatment Plant, more than 10 acres out of the 500 acres is used for vegetable farming and other agricultural activities, by the squatters, the water quality does not meet the standards (WHO, 2006). Water from this polluted plant is used for irrigation while sewage sludge is applied as manure (Westcot, 1997). These wastewater sources consist of thousands cubic liters of industrial and domestic effluents

from industries and residential facilities. A report published in the East Medical Journal stated that quite a considerable number of residents in Nairobi eat highly contaminated vegetables (Kutto *et al*., 2011). Research by Karanja and coworkers showed that vegetables grown along Athi River, Ngong and Wangige rivers and those sold in the market places such as Kawangware, Kangemi and Githurai, contained hazardous chemicals and fecal bacterial (Karanja, *et al.*, 2010). Urban farming activities are commonly practiced in informal settlements and the city suburbs. However, although the dumpsite environments, the sewage treatment effluents, and the effluent from slaughtered houses may look ideal for soil fertility for poor farmers and gardeners they may contain hazardous chemicals and disease pathogens (Gislason & Craig, 2005).

A joint research by the University of Nairobi and Kenyatta University, on the quality of vegetables in neighboring community (Khadiha) of the Kibera slum in Nairobi City and Maili Saba alongside Ngong River found heavy contamination by heavy metals and germs. The contaminants were mainly found in stems and leave of gardened vegetables, and raised serious health concern since the leaves and stems are the most consumed parts of vegetables. Soil and plant samples collected in the study also contained high load bacteriological contaminants (Karanja *et al*., 2010). Microbial contamination was also observed in a study conducted to evaluate the extent of for kales (Vegetables) contamination based on the supply chain to Nairobi and its surroundings (Kutto *et al*., 2011). Water used for irrigation from Ngong River has been blamed for heavy metal and bacteriological contamination.

2.4 Adsorption Isotherms

When the adsorbent and adsorbate come in contact for a sufficient time, they form an equilibrium between the available amount of the pesticide adsorbed (adsorbate) on sediments and

the amount remaining in solution. The equilibrium formed is defined by adsorption isotherm which is a curve that links the equilibrium concentration of a pesticide onto the surface of the sediment/soil to the amount of the pesticide in the solution.

This relationship can be expressed by adsorption isotherm which relates the amount of pesticide adsorbed onto sediment/soil surface and the equilibrium amount of the pesticide remaining in solution at a known temperature. There are many isotherm models use to predict equilibrium characteristics (Foo & Hameed, 2010). However, the four (4) commonly used models are as follows:

(I). Linear model (ii), Irving Langmuir model (iii), Herbert Freundlich model (IV), and the Brunauer, Emmet, and Teller (BET). These common adsorption isotherm models have been used to study adsorption on activated carbon at water and wastewater treatment plants (Thompson *et al.*, 2001). The Herbert Freundlich isotherm is an experimental equation, whereas the Irving Langmuir isotherm is established on rational fundamentals i.e., Langmuir Isotherm considers: a monolayer equilibrium isotherm, making all adsorption sites equally distributed and it obeys 2^{nd} order chemical kinetic parameters. The first and most widely used is the Freundlich Isotherm (Freundlich, 1906). Adsorption isotherm model plays a very important role in adsorption thermodynamic because it states the amount of solute (pesticide) that the sediment/soil surface is capable of adsorbing at equilibrium depending on how much is left in solution.

2.4.1 Freudlich Isotherm

The characteristic adsorption of a pesticide by soils or sediments can be described by the Freundlich empirical isotherm in equation 2.1 (Hutson and Yang, 2000) and it derivation follows from equation 2.2 to equation 2.5.

$$C_{ads} = K_F C_e^{1/n} \ldots\ldots\ldots\ldots\ldots\ldots\ldots\ldots\ldots\ldots\ldots\ldots\ldots\ldots (2.1)$$

Where C_{ads} (q_e) is concentration (milligram/mL) of the amount of pesticide adsorbed and K_F is Freudlich constant. C_e depicts concentration (milligram/mL) of pesticide (solute) in solution as equilibrium is established. The adsorption process of pesticides on soils involves several factors which are considered in conducting adsorption analysis (Vodrais *et al*., 2002).

First, what is the kinetics involved, particularly the amount of adsorption and desorption rate constants and the energy involved. Does the relationship show weak or strong interaction between the solute and the adsorbents? Second, what are the conditions before and at equilibrium and what impacts do the chemical compositions and/or configurations of both (adsorbent and pesticide) affect the result (Bowman and Sans, 1977).

In order to obtain the adsorption, desorption, equilibrium, kinetic and thermodynamic data, it is essential to come up with a functional adsorption/desorption isotherm model which can be used to calculate the relative equilibrium constant and its kinetic information (Srivastava *et al*., 2006). It is assumed that the colloidal/sediment particles adsorb the pesticide (solute) during shaking period, which indicates that the sediment is held in suspension. In such case, the adsorption and/or desorption equilibrium is described by the following equations:

$$nX + S \leftrightarrow SX_n \ldots\ldots\ldots\ldots\ldots\ldots\ldots\ldots\ldots (2.2)$$

$$K = [SX_n]/[X]^n[S] \ldots\ldots\ldots\ldots\ldots\ldots\ldots\ldots (2.3)$$

$$[SX_n] = K[X]^n[S] \ldots\ldots\ldots\ldots\ldots\ldots\ldots\ldots (2.4)$$

Where X is the pesticide molecule of interest; S is the adsorbent/substrate or the point of adsorption onto the surface of the colloid and/or sediment particle in solution and K is

desorption/adsorption equilibrium constant. Whereas SXn is the particle-pesticide adsorption complex formed. Similarly, one can note that S is a solid whose mass is very large compared to the solute. Therefore, [S] can customarily be taken to be unity, hence reducing Equation (2.4) to:

$$[SX_n] = K[X]^n \ldots\ldots\ldots\ldots\ldots\ldots\ldots (2.5)$$

$$C_{ads} = K_F C_e^n \ldots\ldots\ldots\ldots\ldots\ldots 2.6$$

Taking log of both the left hand side (LHS) and right hand side (RHS) we have:

$$\log[SX_n] = logK + nlog[X] \ldots\ldots\ldots\ldots\ldots (2.7a)$$

$$lnq_e = lnK_F + 1/lnC_e \ldots\ldots\ldots\ldots\ldots\ldots\ldots (2.7b)$$

Since Equation (2.6) is linear, the K value of the equilibrium constant, and n (number of pesticide molecules) can be obtained from the slope and intercept of log [SXn] versus log[X] plot, respectively. In addition, the standard Gibbs free energy of activation, (ΔG) can be approximated by use of the conventional equation:

$$K = e^{-\frac{\Delta G}{RT}} \ldots\ldots\ldots\ldots\ldots\ldots\ldots\ldots\ldots\ldots (2.8)$$

Considering the assumption that colloid and/or sediment adsorb Lambda-Cyhalothirn at the time of shaking (suspended particles) and that these adsorbed pesticide substrates melt onto the surfaces of the sediment as it settles. This means, at that moment the amount of reagent substrates (Lambda-Cyhalothrin) adsorbed by suspended particles, i.e. $[X]_{ads}$ is found from Equation (2.8):

$$[X]_{ads} = [X]_i - [X]_e \ldots\ldots\ldots\ldots\ldots\ldots (2.9)$$

Where $[X]_i$, represents the initial pesticide concentration before the addition of a known mass of sediments and $[X]_e$ is the equilibrium pesticide concentration. Also agitation enables the settling of sediments hence the separation of both adsorbed and dissolved pesticide particles. Since n,

number of pesticide particles is related to a sole adsorption point, [SXn] is obtained by:

$$[SX_n] = \frac{1}{n}([X]_i - [X]_e) \ldots\ldots\ldots\ldots\ldots\ldots\ldots\ldots\ldots (2.10)$$

$$[SX_n] = \frac{1}{n}[X]_{ads} \ldots\ldots\ldots\ldots\ldots\ldots\ldots\ldots\ldots\ldots\ldots (2.11)$$

This demonstrates the presence of a colloidal bound fraction amid the pesticide and the liquid holding the sediment when it is shaken.

Similarly, they showed that such suspended bound fraction after settling is significantly small relative to sediment bound fraction which justifies the early statement made concerning how to find [SXn] using $[X]_{ads}$ as stated above. It should be noted that [SXn] is the equilibrium amount of suspended colloidal bound fraction at settling since not all the pesticide were adsorbed. Therefore, on modifying Equation (2.11) to show the total adsorbed pesticide, we have:

$$[X]_{ads} = nK'([X]_e + [SX_n]_w)^n \ldots\ldots\ldots\ldots\ldots\ldots (2.12).$$

From above in Equation (2.11), K' represents the apparent adsorption constant while $[SX_n]_w$ represents amount of colloidal bound fraction as it slows down at equilibrium. When the natural logarithm is taken, Equation (2.12) yields a linear expression:

$$\ln[X]_{ads} = \ln(nK') + nln([X]_e + [SX_n]_w \ldots\ldots\ldots\ldots\ldots (2.13)$$

If equilibrium is formed between the sediment (colloidal bound fraction) and the one in suspension Equation (2.13) becomes:

$$nX + S \leftrightarrow (SXn)w \leftrightarrow (SXn) \ldots\ldots\ldots\ldots\ldots (2.14)$$

It is seen from Equation (2.13) that a state of balance exists in line with [SXn] at settling equilibrium. Additionally, a graph of $ln[X]_{ads}$ versus $ln([X]_e + [SX_n]_w)$ as indicated by Equation (2.12) does not impact the result of n in Equations (2.6 and 2.10) thus it impacts result of nK. Therefore, the result of K is not the actual equilibrium constant, rather its relative

equilibrium constant.

2.4.2 Langmuir Isotherm

Langmuir Isotherm predicts that adsorption of the pesticide molecules takes place on uniform surface of monolayer in which there is no interaction between the adsorbate and the energies involved (Langmuir, 1916). It is expressed as shown in Equation 2.15:

$$Q_e = \frac{q_m b C_e}{1 + bC_e} \ldots\ldots\ldots\ldots\ldots\ldots\ldots\ldots\ldots\ldots\ldots\ldots\ldots\ldots (2.15)$$

From Equation 2.15, Q_e stands for the amount adsorbed, C_e is the adsorbate equilibrium concentration (mg/L) and q_m is the highest amount adsorbed relative to the mass and available adsorption sites. This expression can be linearized as follows:

$$\frac{C_e}{q_e} = \frac{1}{bQ^0} + \frac{C_e}{Q^0} \ldots\ldots\ldots\ldots\ldots\ldots\ldots\ldots\ldots\ldots\ldots\ldots\ldots (2.16)$$

2.4.3 Quasi Langmuir Isotherm

A different circumstance of Langmuir Isotherm termed Quasi-Langmuir is expressed below:

$$q_e = \frac{Q^{\circ} K_L C_e}{1 + K_L\, C_e} \ldots\ldots\ldots\ldots\ldots\ldots\ldots\ldots\ldots\ldots (2.17)$$

The parameters in this equation remain as in the original Langmuir equation. Langmuir is predicated upon three premises: monolayer, site equivalent and site independent. These three conditions are hardly met in sorption at one moment due to physical and chemical characteristics. Modified Langmuir isotherm models come in to account for such missed out conditions. The linear form of the equation 4.4 is expressed as:

$$\frac{1}{q_e} = \left(\frac{1}{K_L Q^0}\right) * \frac{1}{C_e} + \frac{1}{Q^m} \ldots\ldots\ldots\ldots\ldots\ldots\ldots\ldots (2.18)$$

In this linear (Equation 2.18), $1/q_e$ can be plotted against $1/C_e$ that gives a slope at $1/K_L Q^0$ and intercept at $1/Q^0$.

2.4.4 Temkin Isotherm Model

This isotherm model predicts that heat of adsorption of chemical species linearly decreases with respect to adsorbate-adsorbent interactions. This process is a typical even distribution of the bonding energy and it extends to the binding energy (Temkin & Pyhev, 1940). It does not consider the extremely low and large values of concentration though it is a gas phase equilibrium prediction. It emphasizes that adsorption is marked by uniform sharing of the bonding energy up to higher level binding energy (Temkin and Pyhev, 1940). This model is expressed as follows:

$$q_e = \frac{RT}{b_T}\ln(K_T C_e) \ldots\ldots\ldots\ldots\ldots\ldots\ldots\ldots\ldots\ldots\ldots\ldots\ldots\ldots\ldots\ldots (2.19)$$

This equation (Equation 2.19) can be expressed linearly as:

$$q_e = B_T ln K_T + B_T ln C_e \ldots\ldots\ldots\ldots\ldots\ldots\ldots\ldots\ldots\ldots\ldots\ldots\ldots\ldots (2.20)$$

From these Equations (2.19) and (2.20), note that K_T (g/L) is binding constant, R is universal gas constant (J/Kmol), T is absolute temperature (K), b is change in adsorption energy (KJ/mol), and B_T is Temkin equilibrium Constant representing RT/b_T. in Table 4.9, the parameters such as B_T, $B_T lnK_T$, and K_T were obtained from the absorbance extrapolation.

2.4.5 Dubinin-Radushkevich (D-R) Isotherm Model

The model was used to show the apparent adsorption energy heterogeneity at sites of adsorption. This model has fitted well with high solute activities including intermediate concentration range data. This approach was originally applied to differentiate between the physical and chemical adsorptions of metal ions with its main free energy (E) per molecule (Dubinin, 1960). The equation and its linear form are expressed below:

$$ln q_e = ln q_D - B_D \varepsilon^2 \ldots\ldots\ldots\ldots\ldots\ldots\ldots\ldots\ldots\ldots\ldots\ldots\ldots\ldots (2.21)$$

$$\varepsilon = RTln\left[1 + {}^{1}/_{C_e}\right] \ldots\ldots\ldots\ldots\ldots\ldots\ldots\ldots\ldots\ldots\ldots\ldots\ldots\ldots (2.22)$$

From the above expressions, q_D is adsorption strength of soil/sediment (mg/g), B_D is Dubinin-Radushkevich constant, q_e is amount of adsorbate at equilibrium (mg/g), and E is the free energy per molecule of adsorbate. T is the absolute temperature (k), R is the universal gas constant (j/kmol) and C_e is the adsorbate equilibrium concentration (mg/L).

One unique characteristic of this model is that it is temperature dependent. This allows for all suitable data to lie in the same curve, characteristic curve when adsorption data at separate temperatures are plotted as function of the amount adsorbed (lnqe) against the energy (E).

CHAPTER THREE

3. MATERIALS AND METHODS

3.1 Area of Study and Collection of Samples

The sediments used in this study were collected along Athi River at three (3) sampling sites representing the upstream (Site 1), midstream (Site 2), and downstream (Site 3), and randomly selected soil samples from Athi River (Site 4) and Kwale. The collected samples were placed in sample bags and transported to the laboratory, department of Chemistry, University of Nairobi for analysis. The samples were dried and crushed into fine particles.

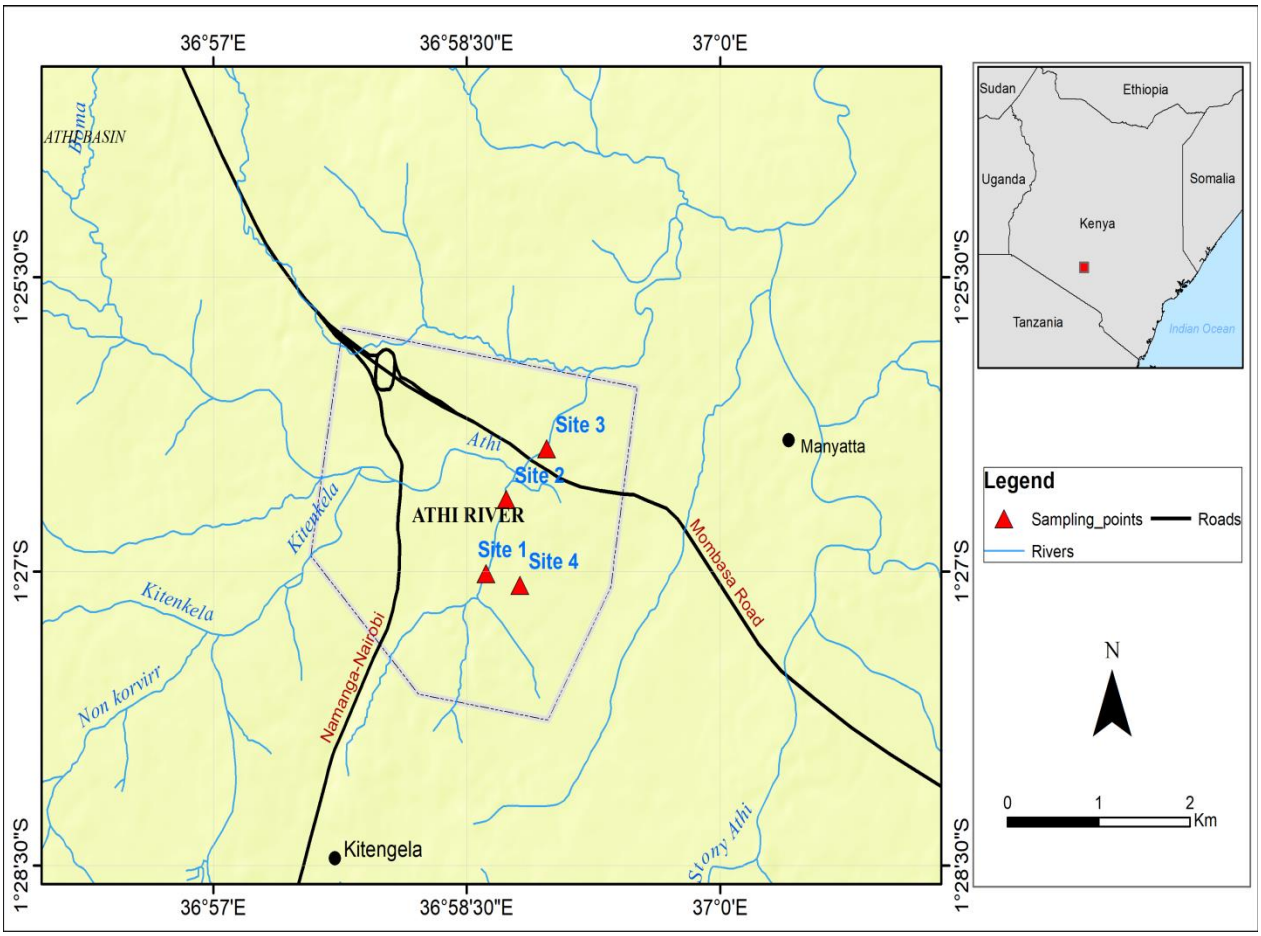

Figure 3. 1: Study Area.

3.2 Apparatus and Instrumentation

The following materials, instruments and reagents were used:

UV-Visible spectrophotometer (UV-1700 Schamadzu model), Mini Orbital Shaker, Analytical balance (Fischer scientific A-160), Lambda-Cyhalothrin (karate 25g/kg pure), Glass bottles, Distilled water, Stop watch, Acetone and River sediment from Athi River and kwale coastal soil, in Kenya.

3.3 Chemicals and Reagents

3.3.1 Determination of Available Soil/Sediments Nutrients (Ca, K, Mg, Mn, Na and P)

The oven-dried soil samples were extracted in a 1:5 (mass/volume) ratio and combined with dilute hydrochloride acid (0.1N) and Sulfuric acid (0.025 N), respectively, (Carter, 1993). The determinations of metallic elements including sodium (Na), calcium (Ca), and potassium (K) were carried out using flame photometry while others, phosphorous, magnesium and manganese were determined calorimetrically (Mehlich, 1953).

3.3.2 Determination of Organic Carbon

The available organic carbon content of the samples was oxidized in concentrated dichromate solution at 150 ^{0}C for half an hour to be oxidized completely. The digest was cooled and Barium chloride added. The digests were mixed thoroughly and placed in a controlled environment for a 12-hour period undisturbed. The concentration was analyzed using spectrophotometer at a range between 200-900 nm (Gislason & Craig, 2005).

3.3.3 Total Nitrogen

The soil samples were digested with Conc. Sulphuric acid which contained selenium, potassium sulphate and copper sulphate and hydrated at about 350 ^{0}C. Total elemental Nitrogen (N) content

was determined by Distillation followed by Titration with the sulfuric acid (H_2SO_4) solution (Persson *et al*., 2008).

3.3.4 Soil pH Determination

The pH of the soil was determined in a 1:1 ratio of soil to water (weight/volume) using pH meter.

3.3.5 Trace Elements Analysis

The soil sample was oven-dried and obtained in a ratio of 1:1 (weight/volume) using dilute Hydrochloride (0.1M) extract to determine trace elements such as Fe, Zn and Cu using an Atomic Absorption Spectrophotometry, (FAAS) (Yang and Chang, 2005).

3.3.6 Cation Exchange Capacity at Neutral pH (Ca, Mg, K, and Na)

The samples were extracted with a dilute ammonium acetate solution (1N) buffered at neutral pH. The filtrate cation exchanged capacity for exchangeable metallic elements including Calcium, Magnesium, Potassium and Sodium were analyzed. The samples were leached again this time, with 1N KCl, and the leachates were used for the determination of the Cation Exchange Capacity. The expected elements such as sodium and potassium were determined using a flame photometry while others like calcium and magnesium were determined using the Flame Atomic absorption spectrophotometry. This was followed by the determination of Cation Exchange Capacity through Distillation followed by Titration with 0.01MHCl (Carroll, 1959); (Tuner and Clark, 1966).

3.4 Preparation of Standards and Reagents

3.4.1 Preparation of Standard Reagents

A standard solution of L-Cyhalothrin (1000 mg/L) was prepared and through appropriate dilution, the following concentrations were made: 2, 4, 6, 8, 10, 20, 40, 60, 80, and 100mg/L. Absorbance for these dilute solutions were obtained photometrically at a range between 200 to 900nm to obtain the lambda maximum. To investigate the existence of the adsorption/desorption equilibrium, 2.0g, 1.0g, 0.5g, 0.2g and 0.1g of the dried sediments were placed in glass bottles and shaken with 10 ml of 1mg L-Cyhalothrin solution for an hour. The pesticide containing solutions were given about seventy two (72) hours to settle down. The aqueous parts were poured and filtered with a Whitman filter paper to obtain a clear conc. L-Cyhalothrin solution. The absorbance of C_e and Q_e was obtained using a UV-Visible spectrophotometer at 218 nm. To find ΔG, n and K, a 0.5g of the samples were mixed and shaken with 10ml deionized water spiked at 50, 40, 30, 20, and 10ppm of L-Cyhalothrin. The samples, each in a set of three (3) were shaken for 15min, 30min, 45min and 60min using an orbital shaker. Similarly, the concentration of L-Cyhalothrin in the decanted solution was obtained as explained above.

3.5 Degradation Procedure

In the degradation, a set of 3 experimental samples of 5g each (Athi River and Coastal soils) were weighed. To each, a concentration of 50 mg/L of L-Cyhalothrin was added in 100-ml glass bottles. The samples were stored in the dark and monitored on weekly interval for a period of five weeks. At each monitoring interval, like in the adsorption, the solution was decanted, filtered and run at 218 nm using UV-spectrophotometry to determine the level of degradation.

CHAPTER FOUR

4. RESULTS AND DISCUSSION

4.1 Sediments and Soil Characterizations

Characterization of both Athi River soil and sediments including Kwale soil was done using standard methods of soil analysis. The results of the analysis are in Tables 4.1 and 4.2.

Table 4.1: Athi River Sediment Profile used in the Adsorption Analysis.

Field	**Upstream**	**Midstream**	**Downstream**
Sediment depth	2-5cm	2-5cm	2-5cm
Parameters	**Value**	**Value**	**Value**
pH	6.47	7.59	7.68
Total Nitrogen (%)	0.08	0.11	0.10
Total Org. Carbon (%)	0.54	0.91	0.75
Phosphorus (µg/g)	8.00	11.00	40.00
Potassium me %	0.82	1.06	0.60
Calcium me%	23.90	30.20	5.10
Magnesium me%	3.28	3.36	1.76
Manganese me%	2.12	2.68	0.61
Copper (µg/g)	1.56	1.55	1.71
Iron (µg/g)	191.00	174.00	39.30
Zinc (µg/g)	5.00	5.94	2.04
Sodium me%	1.00	1.29	0.50
Electrical Conductivity	0.93	0.86	N/A

The sediments/soils' properties have significant impacts on its adsorption capacity as shown later. The profile of Athi River sediments are shown in Table 4.1. The sediments were sampled about 2-5cm below the surface and one kilometer (1-Km) apart. The pH of the sediments is

generally high above the optimum level for many soils (5.5-6.5). This could be due to a number of factors such as discharges from industries upstream of the river. The high pH could also be attributed to pollution from agricultural activities and waste water discharges into river from surrounding local communities.

From Table 4.1, the primary essential elements (N, P, and K) responsible for soil fertility were low whereas the secondary essential elements (Ca, Na, Mg, Mn, and Zn) responsible for adsorption were higher in the soil. This explains the significance of pH values, i.e., the higher the pH the more dissolved ions, hence the more the adsorption capacity of the sediments especially for halogenated contaminants like pesticides. Another important observation from Table 4.1 is the low amount of available Total Organic Carbon. This was because the samples were collected along the river and as such microorganisms responsible to build such nutrients could be few or completely absent as result of pollution or industrial discharge mentioned earlier. Like Nitrogen, Total Organic carbon plays an important role in adsorption. The Total organic carbons content for all the three sampling sites were 0.54, 0.91 and 0.75% (Table 4.1). This means that the adsorption capacity of these materials is generally low. Another factor that influences the adsorption is the physical dipole-dipole attraction (Van der Waals force) that improves the adsorption capacity for the soil. Similarly, the properties of Athi River and Kwale soils (Table 4.2) exhibited different characteristic values, though degradation of Lambda-Cyhalothrin in both soils behaved similarly.

pH value for Kwale soil was higher than Athi River soil. This high pH could be as a result of relatively low rainfall associated with the coastal region where there is no leaching of the salts in the soil. The total organic carbon content is low probably due to absence of microorganisms.

Table 4.2: Athi River and Kwale Soils used in degradation.

FIELD	**ATHI RIVER SOIL**	**KWALE SOIL**
Soil depth	5-10cm	5-10cm
Parameters	**Value**	**Value**
pH	5.13	7.90
Total Nitrogen (%)	0.90	0.06
Total Org. carbon (%)	1.68	0.50
Phosphorus (µg/g)	33.44	19.00
Potassium me %	1.04	0.29
Sodium	0.18	0.49
Calcium me %	22.61	2.20
Magnesium me %	4.72	1.32
Manganese me %	0.13	0.94
Copper(µg/g)	0.96	1.40
Iron (µg/g)	0.54	2.07
Zinc (µg/g)	40.46	1.78

4.2 Absorption Profile of Lambda-Cyhalothrin

The prepared standard solution of Lambda-Cyhalothrin compared with the literature λ max 218 nm. Figures 4.1 and 4.2 show the UV-Visible spectra range between (0-10 mg/L) and (0-100 mg/L), respectively. The plots of absorbance against concentration at 218 nm gave linear relationship as seen in Figures 4.3 and 4.4.

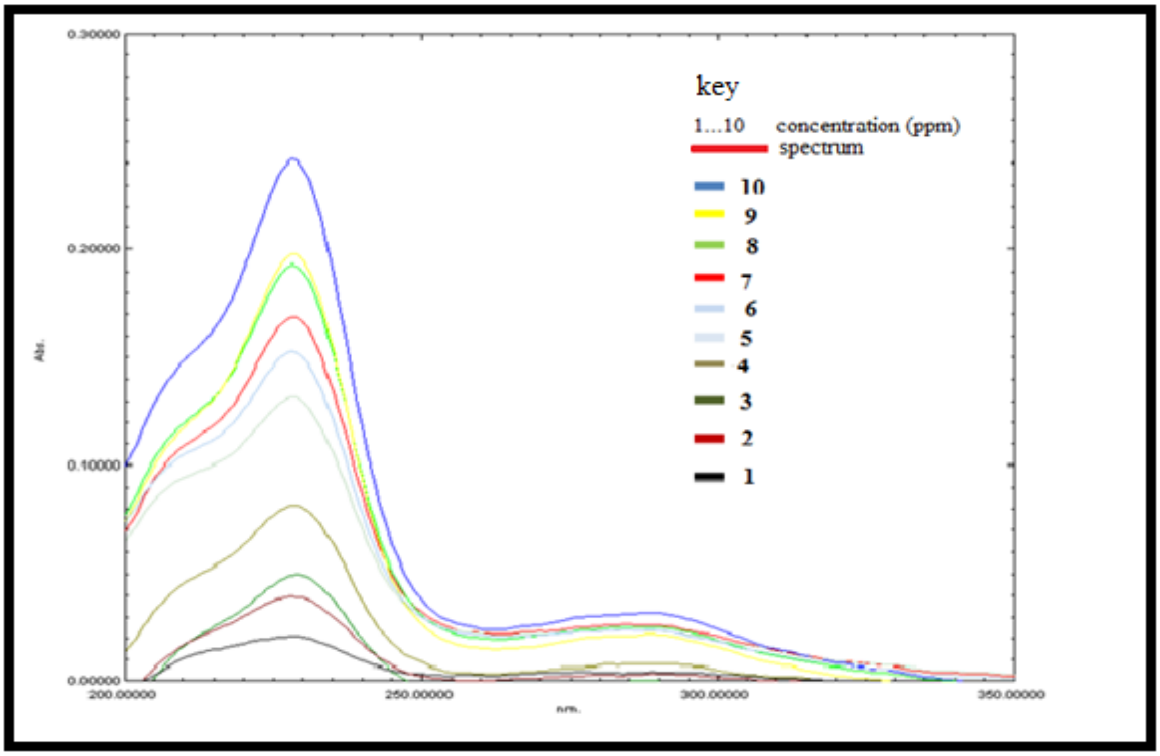

Figure 4. 1: UV- Visible Spectra for L-Cyhalothrin (0-10 mg/L).

Figure 4.2 shows UV-Visible spectra of L-Cyhalothrin range (0-100 mg/L).

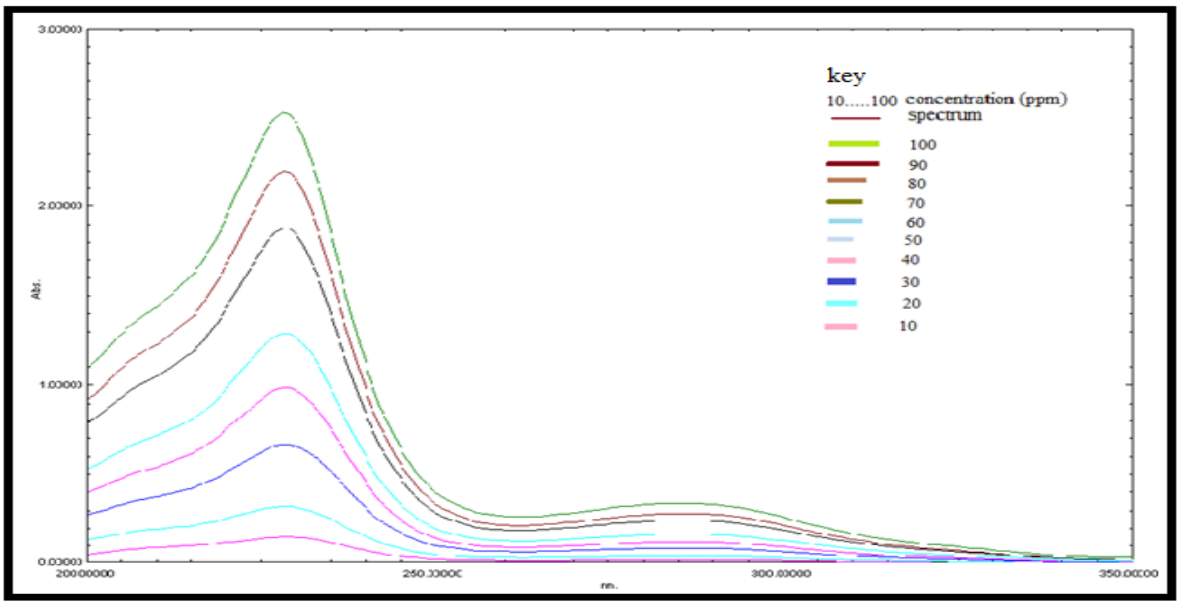

Figure 4. 2: UV-Visible Spectra of L-Cyhalothrin (0-100 mg/L).

This means that Beer's Law was obeyed according to the equation:

$$A = \varepsilon CL \ldots\ldots\ldots\ldots\ldots\ldots\ldots\ldots\ldots\ldots\ldots\ldots\ldots\ldots\ldots\ldots\ldots\ldots . (4.1)$$

Where A is the absorbance, L is the path length of the light (1 cm) and C is concentration. The symbol έ, is the molar absorption coefficient for the chemical species of interest.

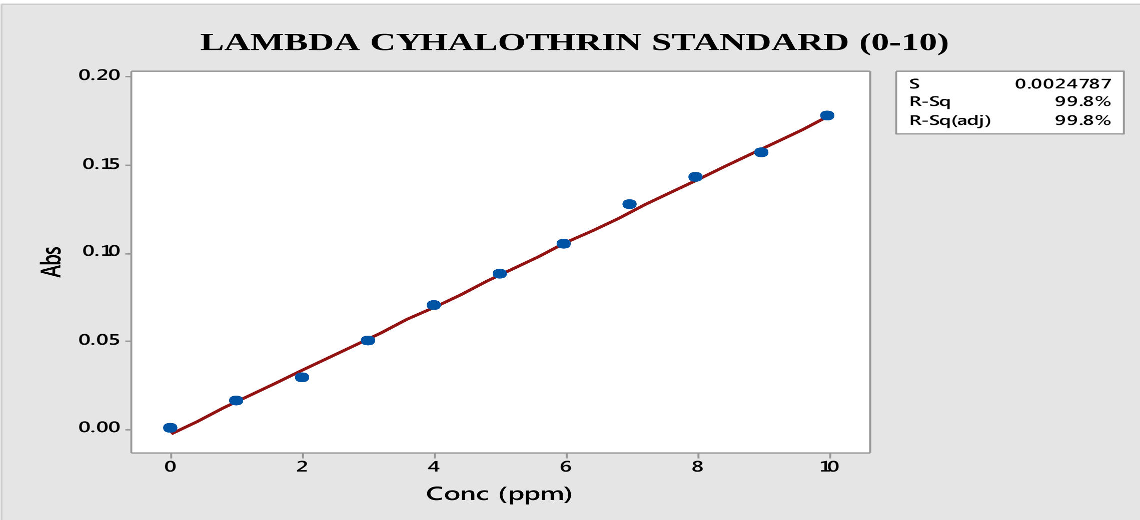

Figure 4. 3: Plot of Absorbance against Concentration (0-10 mg/L) of L- Cyhalothrin.

Figure 4.4 is the linear plot of Figure 4.2, i.e., absorption spectra of L-Cyhalothrin (0-100 mg/L).

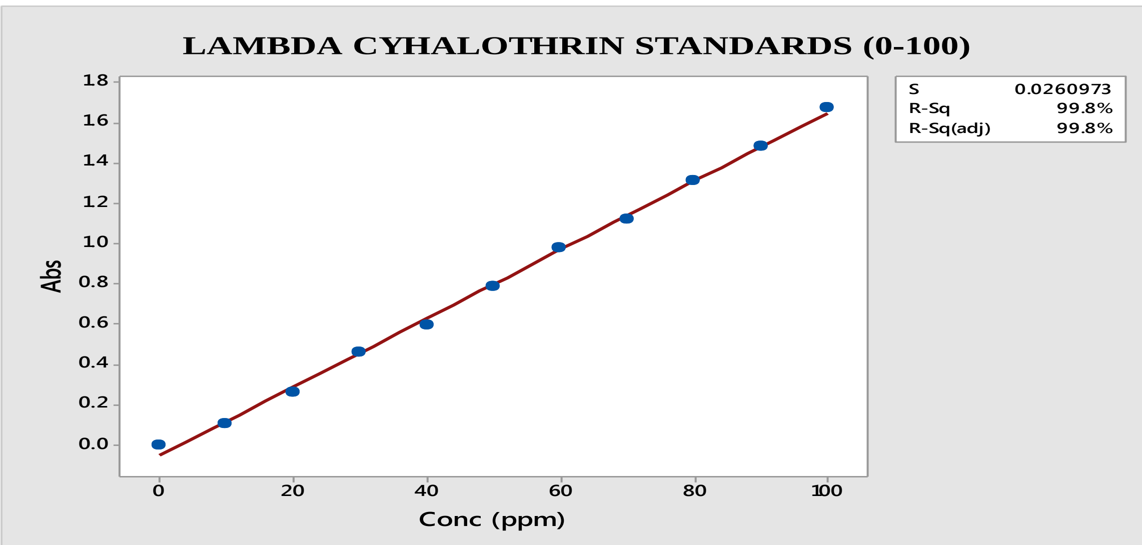

Figure 4. 4: Plot of Absorbance against Concentration (0-100 mg/L) of L-Cyhalothrin.

4.3 Effect of Sediment Mass

The adsorption level of varied amounts of sediment masses as function of the concentration of Lambda-Cyhalothrin are given in Figures 4.5 and 4.6. It was established that the larger the amount of sediment, the lower the amount of lambda-Cyhalothrin (Pesticide) in the solution. This showed that as the number of available adsorption sites (sediment) increased the more it removed the pesticides from the solution, obeying the predictions of the isotherm models (Freundlich, Langmuir and others). As the mass of the sediment increased more adsorption sites, the average amount of L-Cyhalothrin adsorbed increased for all samples. For example in sample C (Downstream sediment), the average amount of L-Cyhalothrin remaining in solution after adsorption were 3.90, 3.20, 2.20, 1.600 and 0.90 from the initial Conc. (10 mg/L) for sediment masses of 0.10 g, 0.20 g, 0.50 g, 1.00 g and 2.00 g, respectively.

This means the more absorption sites the more molecules of L-Cyhalothrin could be adsorbed. Figure 4.6 gives the adsorption graph of L-Cyhalothrin in the solution measured at same fixed Conc. and time against varied masses.

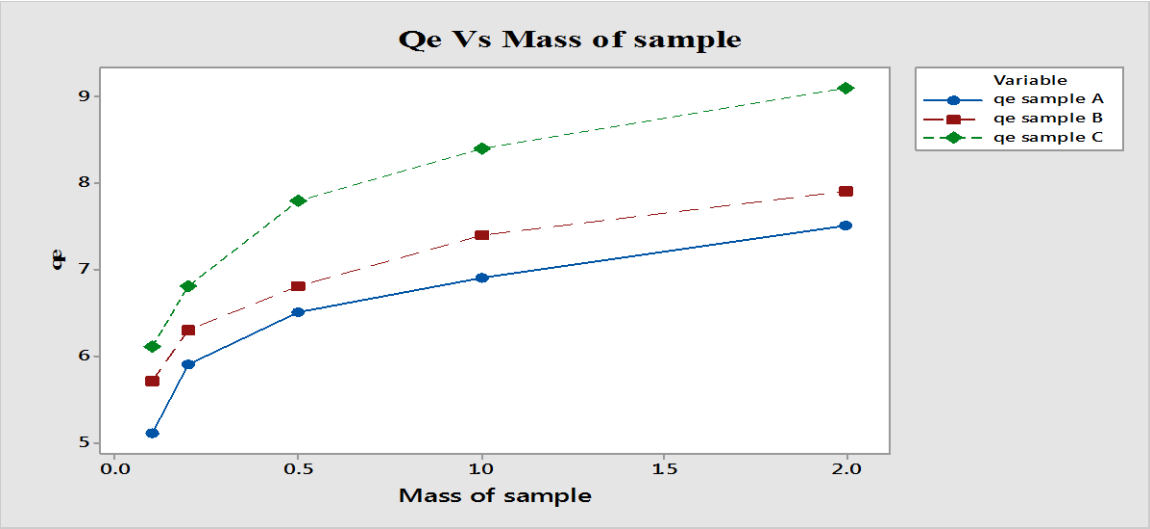

Figure 4. 5: Plot of amount L-Cyhalothrin adsorbed (q_e) vs. varied masses (g) of the sample.

Figure 4.6 gives the desorption graph of L-Cyhalothrin in the solution measured at fixed Conc. and time against varied masses.

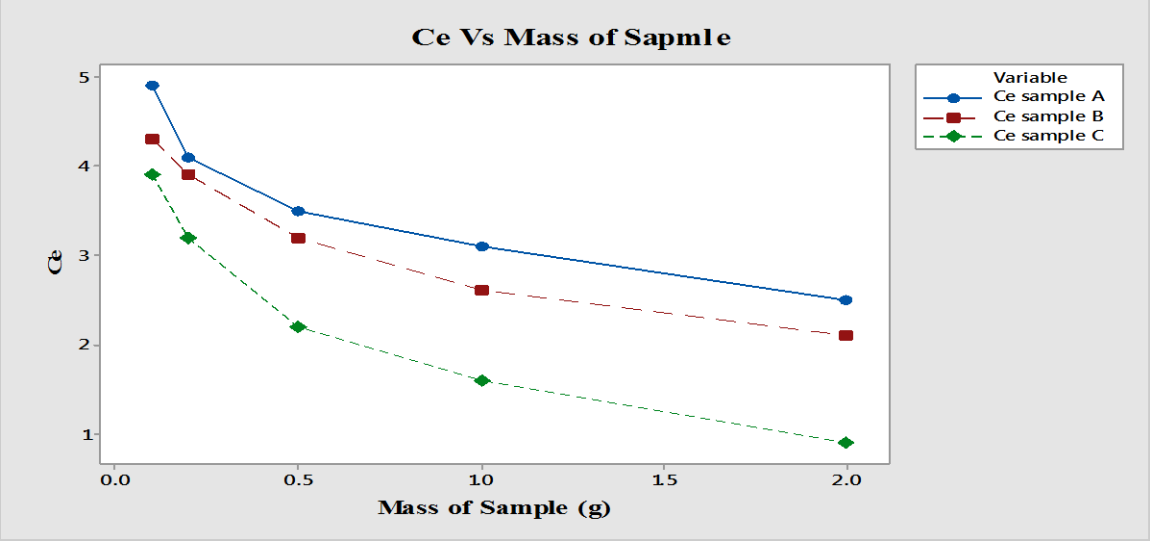

Figure 4. 6: Plot of amount in solution (C_e) against varied masses (g) of the sediment.

From Figures 4.5 and 4.6, samples A, B, and C mean Upstream (A), Midstream (B), and Downstream (C) of Athi River, respectively. Whereas q_e is the equilibrium concentration of the solute and C_e is the concentration of Lambda-cyhalothrin in the solution. The two graphs for adsorption (Figure 4.5) and desorption (Figure 4.6) revealed reverse behavior for the concentration adsorbed and the concentration remaining in solution, respectively.

4.4 Effect Contact Time

The statistics adsorption results for the three (3) sediments (Upper, Middle and Down streams) of Athi River are shown in Table 4.3. The results obtained from spiking of various concentrations, .i.e, 10 ppm, 20 ppm, 30 ppm, 40 ppm, and 50 ppm of Lambda-Cyhalothrin in 0.5 g of soil at different shaking times and initial pesticide concentrations were calculated from their absorbance relative to the standard solution as shown in Table 4.3.

Table 4. 3: Data Summary for Adsorption Parameters

N0	Shaking Time (Minute)	Initial Conc.	SAMPLE A		SAMPLE B		SAMPLE C	
			C_e	Q_e	C_e	Q_e	C_e	Q_e
1	15	10	1.97 ± 0.02	8.03	2.07 ± 0.02	7.93	3.61 ± 0.08	6.39
2		20	2.63 ± 0.03	17.37	3.03 ± 0.04	16.97	3.83 ± 0.01	16.17
3		30	2.89 ± 0.01	27.11	3.21 ± 0.02	26.79	4.37 ± 0.04	25.63
4		40	6.50 ± 0.02	33.50	6.90 ± 0.03	33.10	6.44 ± 0.03	33.56
5		50	8.22 ± 0.31	41.78	8.10 ± 0.03	41.90	6.90 ± 0.14	43.10
6	30	10	1.77 ± 0.02	8.23	1.97 ± 0.02	8.03	3.43 ± 0.07	6.57
7		20	2.77 ± 0.06	17.23	3.50 ± 0.07	16.50	4.03 ± 0.02	15.97
8		30	3.30 ± 0.09	26.70	4.10 ± 0.02	25.90	5.33 ± 0.04	24.67
9		40	5.60 ± 0.04	34.40	4.97 ± 0.13	35.03	6.80 ± 0.17	33.20
10		50	8.87 ± 0.04	41.13	5.83 ± 0.04	44.17	8.00 ± 0.18	42.00
11	45	10	2.07 ± 0.04	7.93	2.20 ± 0.02	7.80	4.13 ± 0.12	5.87
12		20	2.67 ± 0.03	17.33	2.67 ± 0.07	17.33	4.57 ± 0.06	15.43
13		30	3.03 ± 0.04	26.97	3.27 ± 0.07	26.73	4.90 ± 0.03	25.10
14		40	7.23 ± 0.02	32.77	5.77 ± 0.04	34.23	5.47 ± 0.08	34.53
15		50	8.63 ± 0.11	41.37	7.20 ± 0.06	42.80	7.20 ± 0.12	42.80
16	60	10	2.23 ± 0.04	7.17	1.93 ± 0.03	8.07	4.33 ± 0.01	5.67
17		20	2.83 ± 0.05	17.17	2.47 ± 0.05	17.53	4.97 ± 0.03	15.03
18		30	3.17 ± 0.03	26.83	4.00 ± 0.04	26.00	5.30 ± 0.03	24.70
19		40	5.87 ± 0.06	34.13	5.20 ± 0.02	34.80	7.10 ± 0.08	32.90
20		50	8.50 ± 0.02	41.50	6.63 ± 0.04	43.37	7.77 ± 0.05	42.23

From Table 4.3, as the shaking times increased the amount of the pesticide adsorbed increased. Similarly, the amount of pesticide adsorbed (mg/L) also depends on its initial concentration in solution and the amount of adsorption sites (mass of sediment). Therefore, as the initial concentration increases, the amount of pesticide molecules adsorbed increase proportionately per unit mass of the sediment.

The data obtained were fitted to different adsorption isotherm models. It was observed that the data for each of the sites, the Upstream (sample A), Midstream (Sample B) and downstream (Sample C) fitted well for more than one models. The various adsorption isotherm models and characteristic reactions to the samples are as follows.

4.4.1 Langmuir Isotherm Result

Using Langmuir Isotherm (equations 2.16 and 2.16), for example, the values obtained from the adsorption, at 15 minute $C_e/q_e = 0.1636 + 0.0040Ce$. Therefore, from equation 2.16, $1/bQ^0$ was 0.1636 while $1/Q^0$ was 0.004. To find b as in Table 4.4, $1/b * 1/Q^0 = 0.1636$ and $b= 0.0041/0.1636 = 0.02494$. Similarly, $\Delta G = -RTlnKc$, where R is universal gas constant (J/mol*k), T is the absolute temperature (K) and Kc is the equilibrium constant, which, in this case is b. Therefore $\Delta G = - (8.314 *298 * ln0.02494) = 9.1454$ KJ/mol. The data in the table below was arrived at by making assumption that columbic species don't further react with one another (Langmuir, 1916).

Table 4. 4: Langmuir Isotherm Data.

Time (minute)	Sample	$1/Q^0$	B	$1/bQ^0$	R^2	ΔG
15	A	0.00408	0.02494	0.1636	0.047	9,145.42
	B	-0.00063	-0.00323	0.1950	0.001	-14,209.55
	C	-0.06515	-0.111158	0.5861	0.403	-5,442.74
30	A	0.004740	0.03060	0.1549	0.097	8,638.69
	B	-0.03340	-0.10634	0.3141	0.938	-5,552.52
	C	-0.05350	-0.093662	0.5712	0.539	-5,867.05
45	A	0.00519	0.03136	0.1655	0.068	8,577.91
	B	-0.00770	-0.0369	0.2105	0.075	-8,174.86
	C	-0.1226	-0.129052	0.9500	0.414	-5,072.93
60	A	-0.00257	-0.01288	0.1996	0.011	-10,782.59
	B	-0.01167	-0.05474	0.2132	0.295	-7,197.74
	C	-0.1177	-0.113829	1.034	0.512	-5,383.91

From the above data obtained in Table 4.4 ΔG was calculated for each of the samples. ΔG is positive (+) for sample A (Upstream) indicating non-spontaneous desorption process, whereas samples B (Midstream) and C (Downstream) had negative (-) ΔG values indicating that the reaction was spontaneous adsorption process. A plot of C_e/q_e against C_e gave a nearly straight line with an intercept of $1/bQ^0$ as shown in Figures 4.7, 4.8, and 4.9.

Figure 4.7 shows fitting of Sample A (Upstream) adsorption data to Langmuir Isotherm at varied shaking times (15, 30, 45, and 60 minutes). The unparalleled linearity and crossing over of the curve indicate its unsuitability to the model.

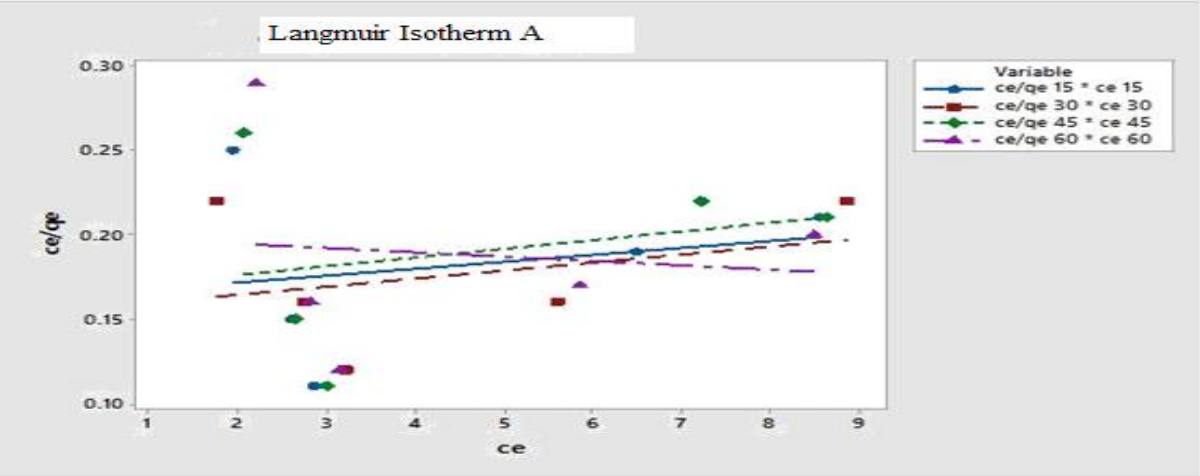

Figure 4. 7: Langmuir Isotherm model for Sample A.

Figure 4.8 also shows the fitting of Sample B (midstream) adsorption data to Langmuir Isotherm at varied shaking times. Similarly, the crossing over indicates unfitting of the data to this model.

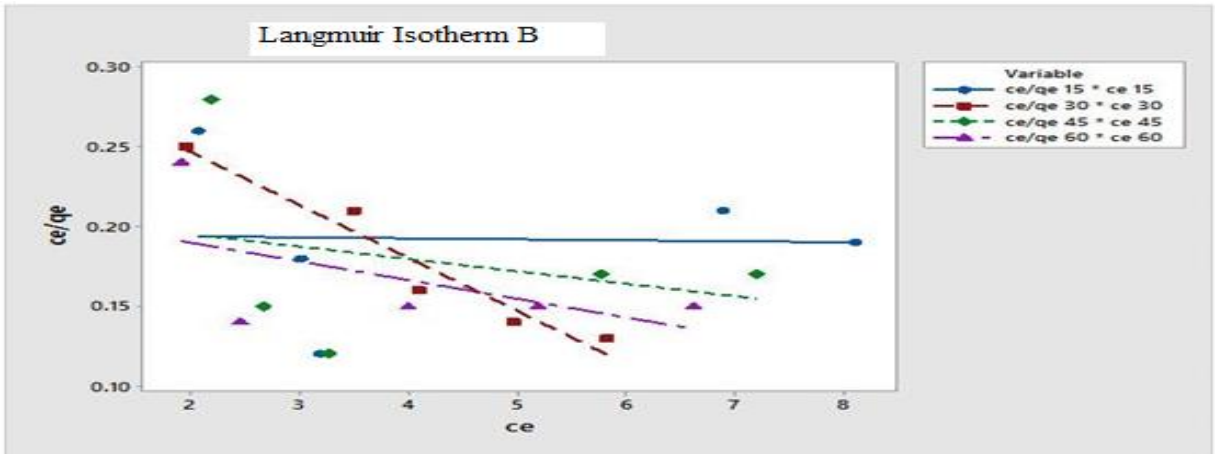

Figure 4. 8: Langmuir Isotherm Model for Sample B.

Similarly as in Figures 4.7 and 4.8, Figure 4.9 shows the fitting of Sample C (downstream) adsorption data to Langmuir Isotherm at varied shaking times. Although the crossing over of the curves looks better fairly but follows similar trends as Figures 4.7 and 4.8.

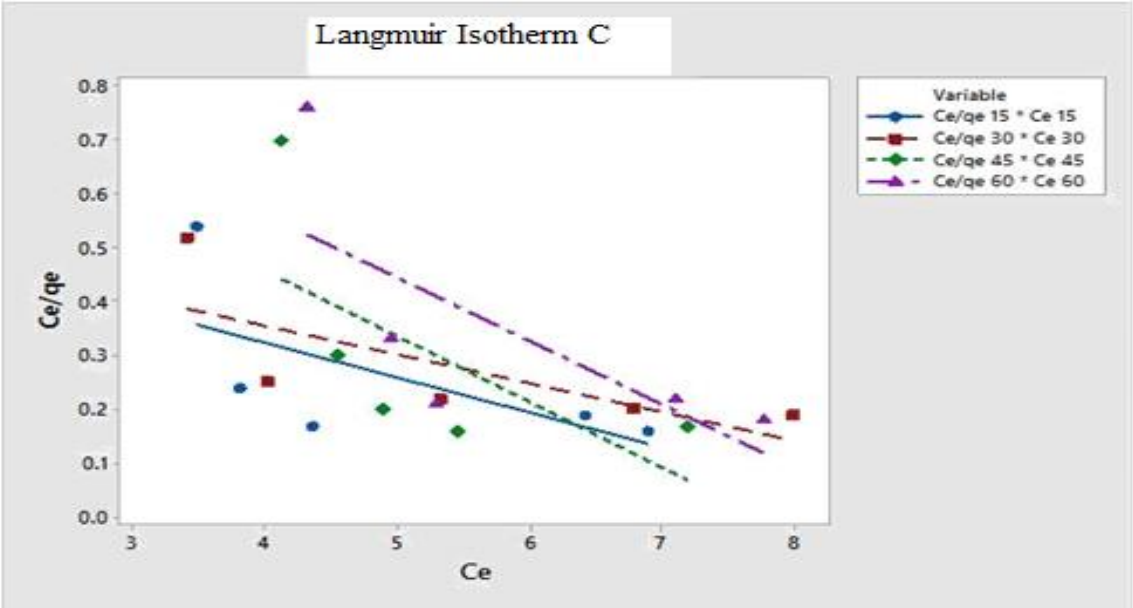

Figure 4. 9: Langmuir Isotherm Model for Sample C.

From the absorbance value obtained at the UV-Visible, C_e was extrapolated using the calibration graph to determine the amount adsorbed from initial concentration added to the sediment. For example, 10 mg/L of Lambda-Cyhalothrin was initially added to sample A (upstream) and shaken for 15 minutes. It was allowed to settle for 72 hours and the clear solution decanted. The absorbance of the solution was measured as 0.915 at 218 nm. The corresponding value deduced from the graph equaling to 4.5 µg/mL (C_e). Plots of C_e/q_e vs C_e were generated as in Figures.4.7, 4.8, and 4.9. A maximum concentration of 10 µg/mL was maintained and the variation in masses (0.1g, 0.2g, 0.5g, 1.0g, and 2.0g) was studied.

4.4.2 Quasi Langmuir Isotherm

A modified Langmuir Isotherm (Equation 2.17 and Equation 2.18) was used to also analyze the adsorption of the sediments from Athi River. In this first modified version of Langmuir, the adsorbate tends to behave as expected as seen from the regression values in Table 4.5. The plots of $1/q_e$ versus $1/C_e$ that has slope at $1/K_LQ^0$ and intercept at $1/Q^0$ of each sample are shown in

Figures 4.10, 4.11 and 4.12.

Figure 4.10 shows the fitting of Sample A (Upstream) adsorption data to Quasi Langmuir Isotherm at varied Conc. and time against fixed mass of the sediment. The data fitted well from the linearity of the Curves and the coefficient of regression (r^2) values in Table 4.5.

Table 4. 5: Quasi-Langmuir Isotherm Data.

Time (minute)	**Sample**	**$1/K_LQ^0$**	**$1/Q^0$**	**K_L**	**R^2**
15	A	0.2165	0.01139	0.52609	0.800
	B	0.2702	-0.01858	-0.0688	0.837
	C	0.6719	-0.0851	-0.12666	0.678
30	A	0.2195	0.01273	0.05799	0.928
	B	0.2937	-0.02881	-0.09809	0.997
	C	0.6969	-0.08077	-0.115898	0.798
45	A	0.2488	0.01567	0.06298	0.766
	B	0.2873	-0.02732	-0.09509	0.759
	C	1.264	-00.1836	-0.145253	0.633
60	A	0.2852	0.02442	0.08562	0.770
	B	0.2422	-0.01963	-0.081048	0.991
	C	1.311	-0.1653	-0.126086	0.712

Figure 4.10 shows the fitting of Sample A (Upstream) adsorption data to Quasi Langmuir Isotherm at varied Conc. and time against fixed mass of the sediment. The curves in this figure are partly linear showing that sediment of Sample A is slightly a better L-Cyhlothrin adsorbent.

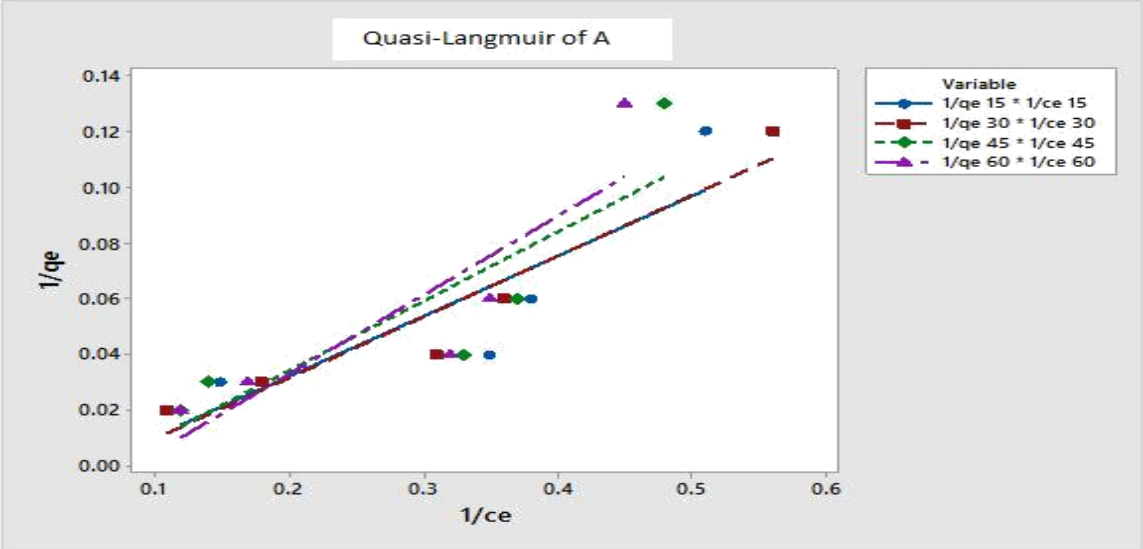

Figure 4. 10: Quasi-Langmuir Isotherm Model for Sample A.

Figure 4.11 shows the fitting of Sample B (Midstream) adsorption data to Quasi Langmuir Isotherm at varied Conc. and time against fixed mass of the sediment. The curves in this figure are more linear than those in Figure 4.10 showing that sediment Sample B is slightly a better L-Cyhlothrin adsorbent than sediment Sample A.

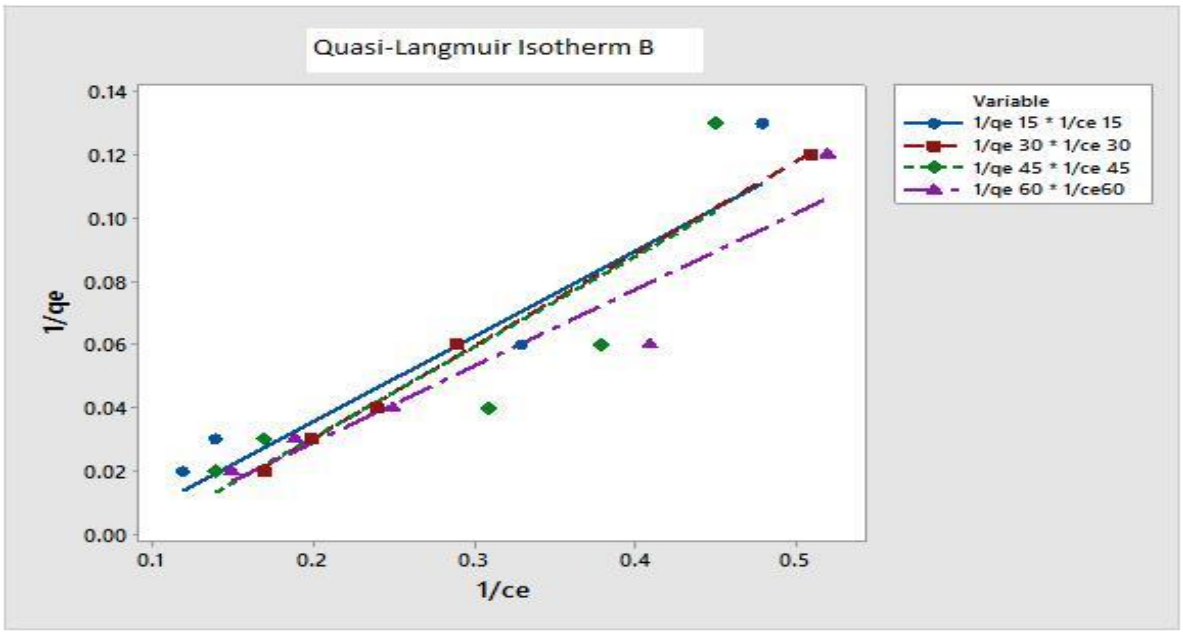

Figure 4. 11: Quasi-Langmuir Isotherm Model for Sample B.

Figure 4.12 like Figure 4.10 and Figure 4.11, shows the fitting of Sample C (Downstream) adsorption data to Quasi Langmuir at fixed mass against Conc. and time. The leaning of the curves shows that the data fitted partly to this model.

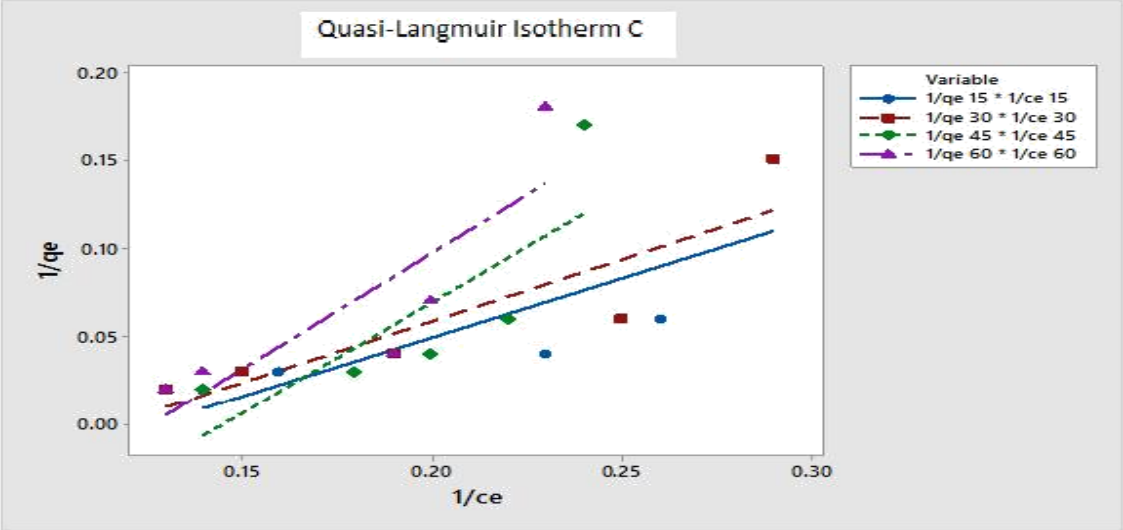

Figure 4. 12: Quasi-Langmuir Isotherm Model for Sample C.

From Equation (4.5), $y = 1/q_e$, $m = 1/K_LQ^0$, $x = 1/C_e$ and $C = 1/Qm$ was used to calculate the regression (r^2) for example at 15 minutes of shaking time: $1/q_e=0.01139+0.2165\ 1/C_e$, $r^2 = 0.80$ and to determine the parameters as in Table 4.7: $1/K_LQ^0 = 0.2165$ and $1/Q^0 = 0.01139$, therefore $K_L = 0.01139/0.2165= 0.52609$ as indicated.

4.4.3 Freudlich Isotherm Model

The same data as in Table 4.6 were exposed to Freundlich isotherm (Equations 2.1 and 2.7b) which gave positive ΔG values for samples C (downstream) and negative ΔG for samples A and B (upstream and midstream, respectively). This means that samples A and B underwent spontaneous adsorption using Freudlich isotherm while sample C went the opposite, non-spontaneous adsorption. Thus the Freundlich Isotherm is characteristic of heterogeneous surface (Freundlich, 1906).

From Equations (2.1 and 2.7b), q_e (mg/g) is the amount of pesticide adsorbed and C_e (mg/L) is the equilibrium concentration. n is a constant that measures the adsorption of non-linearity between the solute concentration in the solution and the adsorption. It (n) expresses parameter that is characteristic of the quasi-Gaussian heterogeneity related to the adsorption surface. K_F (mg/L) is the Freudlich isotherm constant that shows the apparent adsorption capacity of the adsorbent.

Table 4. 6: Freundlich Isotherm Data

Time (minute)	**Sample**	**1/n**	**LnK_F**	**K_F**	**R^2**	**ΔG**
15	A	0.8957	1.883	6.5732	0.754	-4,665.27
	B	1.002	1.691	5.4249	0.829	-1,921.94
	C	2.136	-0.322	0.7247	0.781	797.78
30	A	0.9518	1.834	6.2589	0.861	-4,543.88
	B	1.841	0.5828	1.7915	0.992	-1,444.56
	C	1.966	-0.2400	0.7867	0.904	594.62
45	A	0.8852	1.852	6.3726	0.750	-4,588.48
	B	1.174	1.549	4.7066	0.844	-3,837.67
	C	3.228	-2.2880	0.1015	0.742	5,668.69
60	A	1.053	1.635	5.1295	0.766	-4,050.85
	B	1.249	1.484	4.41055	0.933	-3,676.74
	C	2.930	-2.151	0.1164	0.820	5,329.27

From this equation, plots of $\ln q_e$ versus $\ln C_e$ as presented in this linear form of Freundlich Isotherm have slopes at 1/n and intercepts at $\ln K_F$. Graphs (in Figures 4.13, 4.14, and 4.15) were generated using the data highlighted in Table 4.6 above. Adsorption of Lambda-

Cyhalothrin unto Athi River sediments of the three (3) sampling areas fitted strongly to the Freundlich Isotherm model as shown. The regression (r^2) values ranging from 0.7420 to 0.992 and the linearity of the plot in Figures 4.13, 4.14, and 4.15.

Figure 4.13 shows the fitting of Sample A (Upstream) adsorption data to Freudlich Isotherm at fixed mass against varied Conc. and time. The coefficient of regression (r^2) values and the linearity of the curves show that the data fitted well into Freudlich Isotherm.

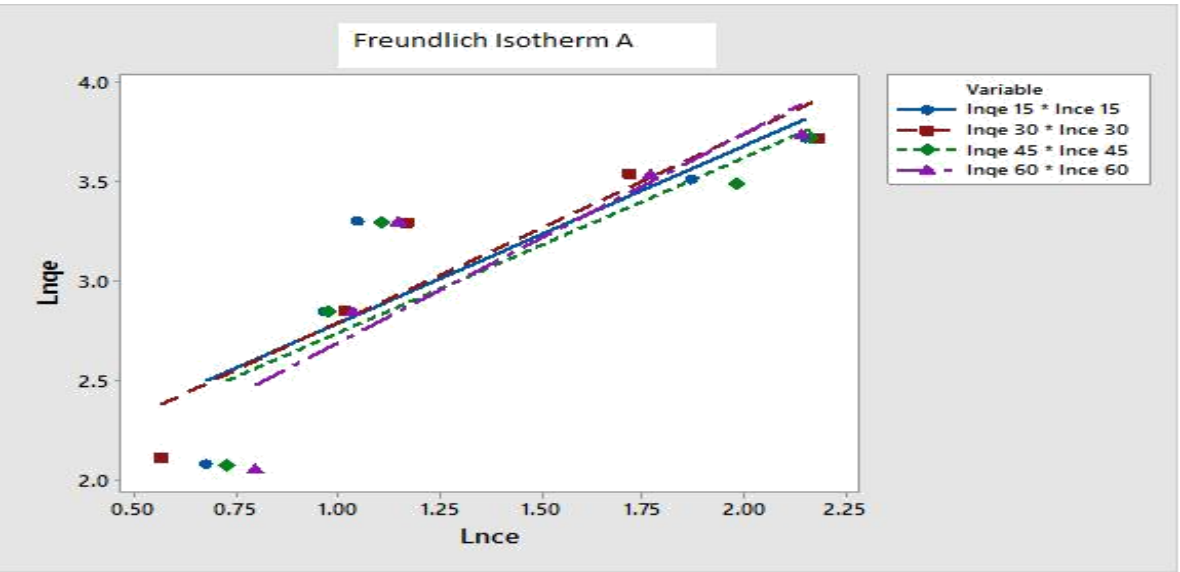

Figure 4. 13: Freundlich Isotherm Model for Sample A.

Figure 4.14 shows the fitting of Sample B (Midstream) adsorption data to Freudlich Isotherm at fixed mass of sediment against varied Conc. (10, 20, 30, 40, and 50 mg/L) and time. Even though there are some crossovers of curves but generally the data fitted well to this model.

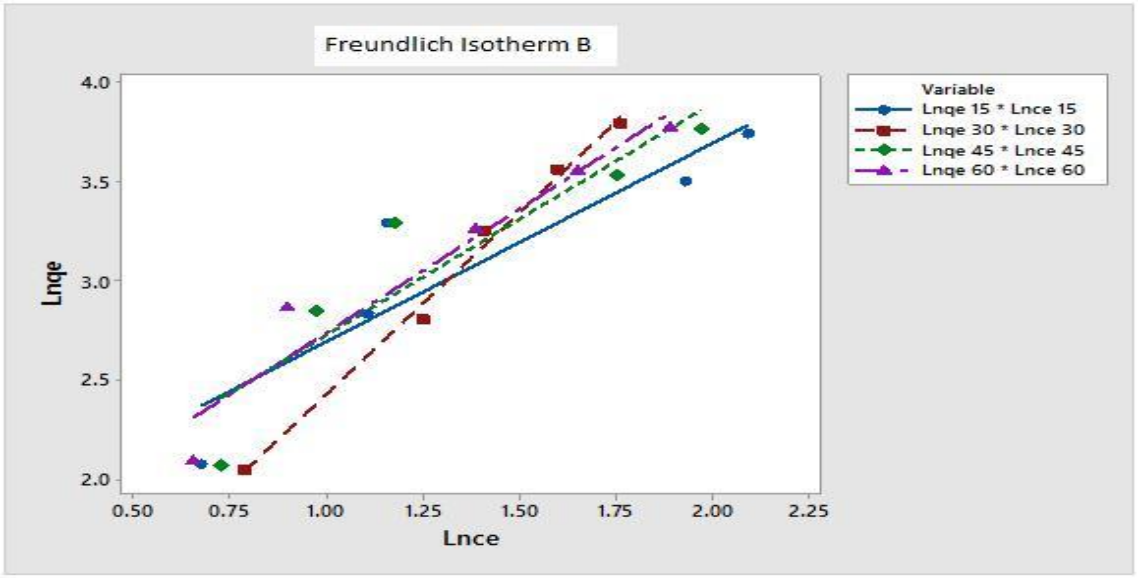

Figure 4. 14: Freudlich Isotherm Model for Sample B.

Similarly, Figure 4.15 shows the fitting of Sample C (Downstream) adsorption data to Freudlich Isotherm at fixed mass against varied Conc. and time. As in Figure 4.13, there is some crossing over of the curves but the data fitted well to the model.

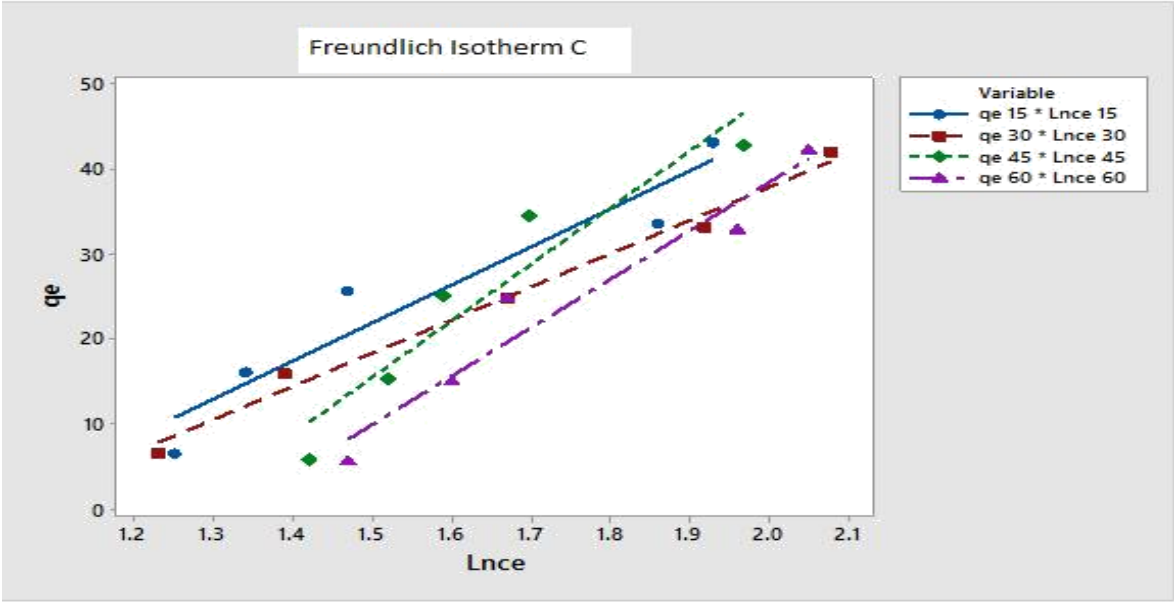

Figure 4. 15: Freudlich isotherm Model for Sample C.

4.4.4 Temkin Isotherm Model

From Temkin isotherm model (Equations 2.19 and 2.20), note that K_T (mg/L) is binding constant, B_T is Temkin equilibrium Constant as in Table 4.9. The parameters such as B_T, $B_T lnK_T$, and K_T were obtained from the absorbance extrapolation. For example, at 30 minutes of shaking time of the Downstream sediment of Athi River, the regression (r^2) = 0.989 was obtained from the q_e = -1.1735 + 20.49 lnC_e 30. From the linear form Temkin isotherm, (equation 4.11), qe = $B_T lnK_T$ + $B_T lnCe$. From this expression, B_T = 20.49, $B_T lnK_T$ = -1.1735, and lnK_T = -1.1735/20.49= -0.084675. Table 4.7 shows the Temkin Isotherm data.

Table 4. 7: Temkin Isotherm Data.

Time (minute)	Sample	B_T	$B_T LnK_T$	K_T	R^2
15	A	19.58	-0.830	0.9585	0.884
	B	0.89	24.10	27.0787	0.002
	C	44.56	-44.97	0.3645	0.916
30	A	20.49	-1.74	0.9188	0.955
	B	-9.45	38.80	-4.1058	0.06
	C	39.11	-40.36	0.3563	0.989
45	A	19.13	-1.35	0.9318	0.871
	B	25.71	-8.23	-0.3195	0.953
	C	66.35	-84.08	0.2816	0.905
60	A	22.95	-6.19	0.7635	0.908
	B	26.59	-8.95	-0.3329	0.982
	C	57.00	-75.64	0.2652	0.947

The graphs generated from the Table 4.7 using Temkin isotherm model are as follow:

Figure 4.16 shows the fitting of Sample A (Upstream) adsorption data to Temkin Isotherm. The data generally fitted very well to this model from the coefficient of regression (r^2) values to the linearity of the curves. The figure shows a fixed mass of sediment Sample A against varied Conc. and time.

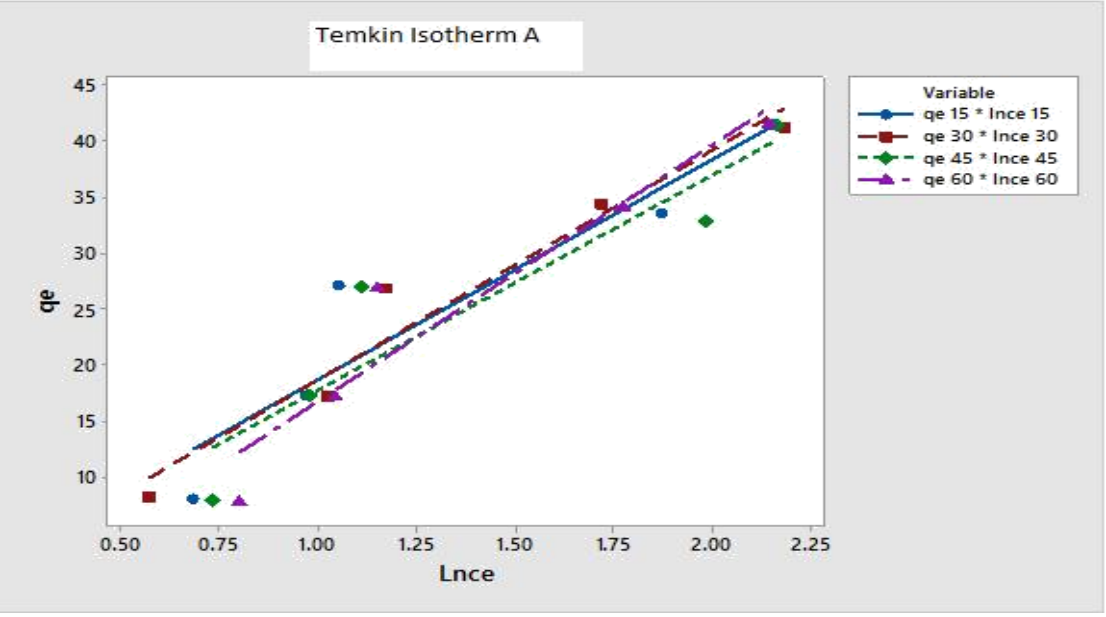

Figure 4. 16: Temkin Isotherm Model for Sample A.

Figure 4.17 shows the fitting of Sample B (Midstream) adsorption data to Temkin Isotherm. As in Figure 4.16, the data fitted well to this model. The curves are well linearized except curves for 15 and 30 minutes of shaking time which could be due to lesser time of shaking.

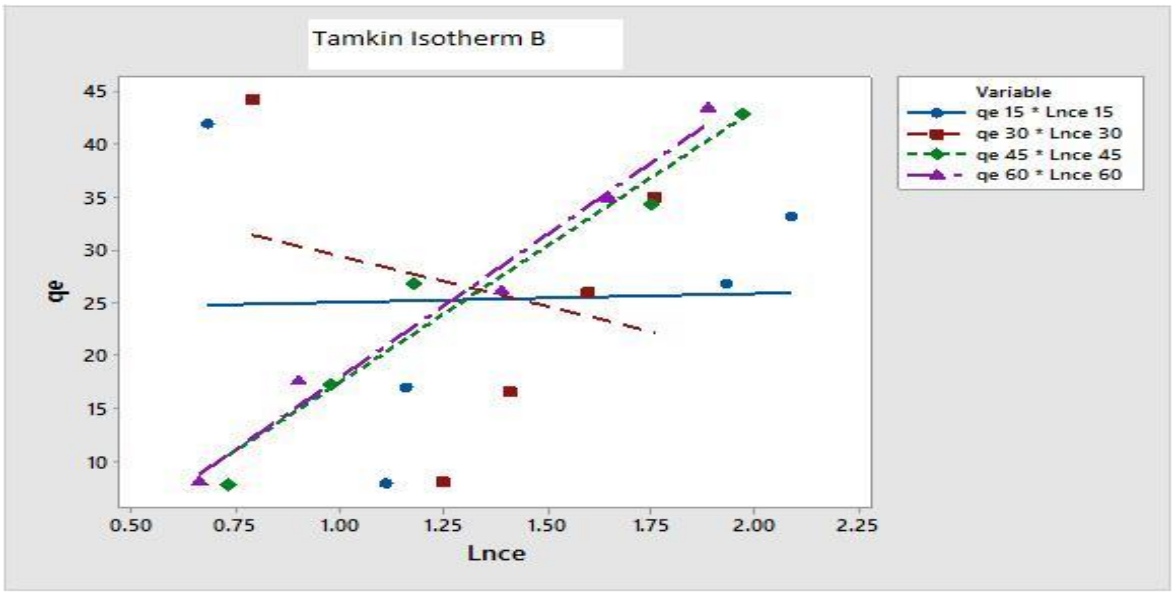

Figure 4. 17: Temkin Isotherm Model for Sample B.

Figure 4.18 also shows the fitting of sediment Sample C (Downstream) adsorption data to Temkin Isotherm. The data gives better coefficient of regression (r^2) in Table 4.7.

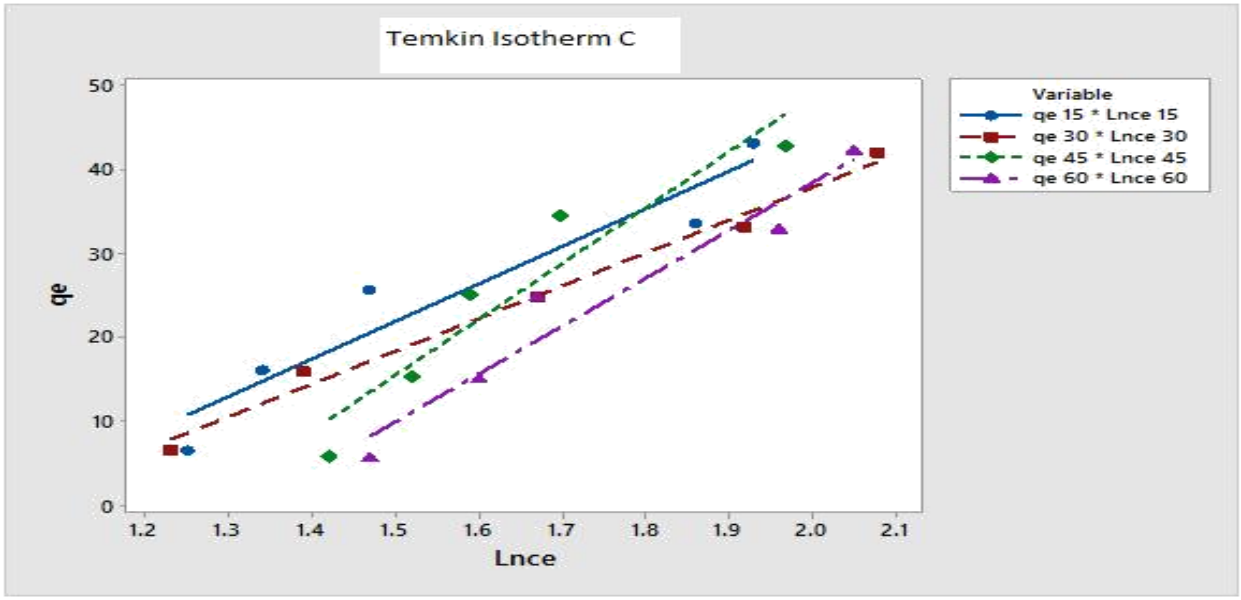

Figure 4. 18: Temkin Isotherm Model for Sample C.

The plots of q_e versus LnC_e from linear expression shown in Equation 4.9 are given in Figures 4.16, 4.17 and 4.18. Samples A and C tend to fit well at different shaking times (15 minutes, 30

minutes, 45 minutes, and 60 minutes) whereas sample B fitted well only at 45 minutes and 60 minutes (Figure 4.16); while 15 and 30 minutes of shaking resulted into disproportionate plots.

4.4.5 Dubinin-Radushkevich (D-R) Isotherm Model

The model was used to show the apparent adsorption energy heterogeneity at sites of adsorption (Equations 2.21 and 2.22). Table 4.8 gives the summarized parameters of D-R data and its graphs in Figures 4.19, 4.20 and 4.21.

Table 4. 8: Dubinin-Radushkevick Isotherm Data

Time (minute)	Sample	Ln q_D	B_D	q_D	R^2	E (KJ/mol)
15	A	3.854	-0.000002	47.1814	0.918	-353,553.39
	B	3.844	-0.000002	46.7120	0.938	-353,553.39
	C	4.421	-0.000006	83.1794	0.864	-117,851.13
30	A	3.795	-0.000001	44.4782	0.980	-707,106.78
	B	3.839	-0.000002	46.4790	0.896	-353,553.39
	C	4.203	-0.000005	66.8867	0.969	-141,421.36
45	A	3.841	-0.000002	46.5720	0.915	-353,553.39
	B	3.995	-0.000002	54.3258	0.941	-353,553.39
	C	5.139	-0.000010	170.5451	0.857	-70,710.68
60	A	3.952	-0.000002	52.0393	0.92.60	-353,553.39
	B	3.888	-0.000002	48.8132	0.975	-353,553.39
	C	4.754	-0.000010	116.0475	0.902	-70,710.68

Figure 4.19 shows the fitting of sediment Sample A (upstream) adsorption to Dubinin-Radushvich Isotherm. The data fitted well to this model. The linear curves and the coefficient of

determination (r^2) values, i.e., 0.918, 0.938, and 0.864 were generated from the plot fixed mass against varied Conc. and time.

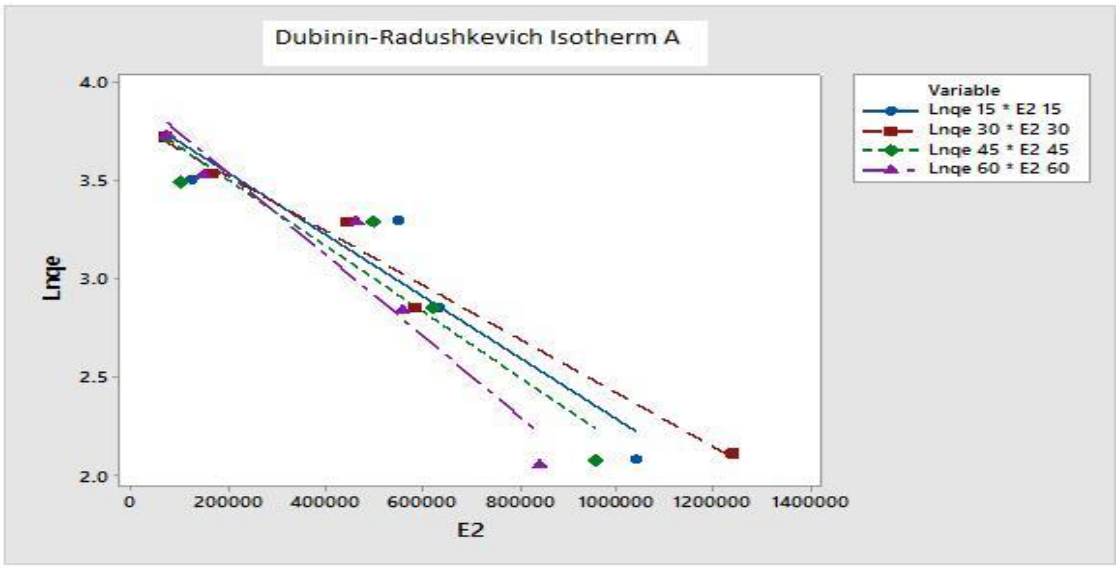

Figure 4. 19: D-R Isotherm Model for Sample A.

Figure 4.20 shows plot of Sample B (midstream) adsorption data to Dubinin-Radushkevick Isotherm. As in Figure 4.19, the data fitted well to this model. The graph faces downward showing amount of L-Cyhalothrin remaining in solution after adsorption.

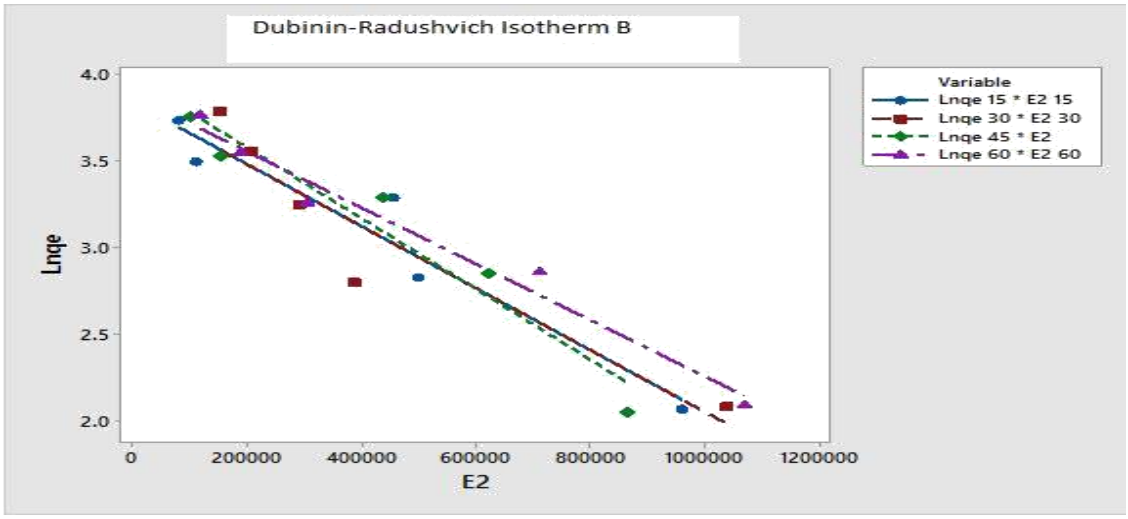

Figure 4. 20: D-R Isotherm Model for B.

Figure 4.21 shows the fitting of sediment Sample C (downstream) adsorption data to Dubinin-Radushkevich Isotherm. The data fitted well to this model though the curves tend to disperse wider as the Conc. of L-Cyhalothrin in solution reduces with increasing free energy.

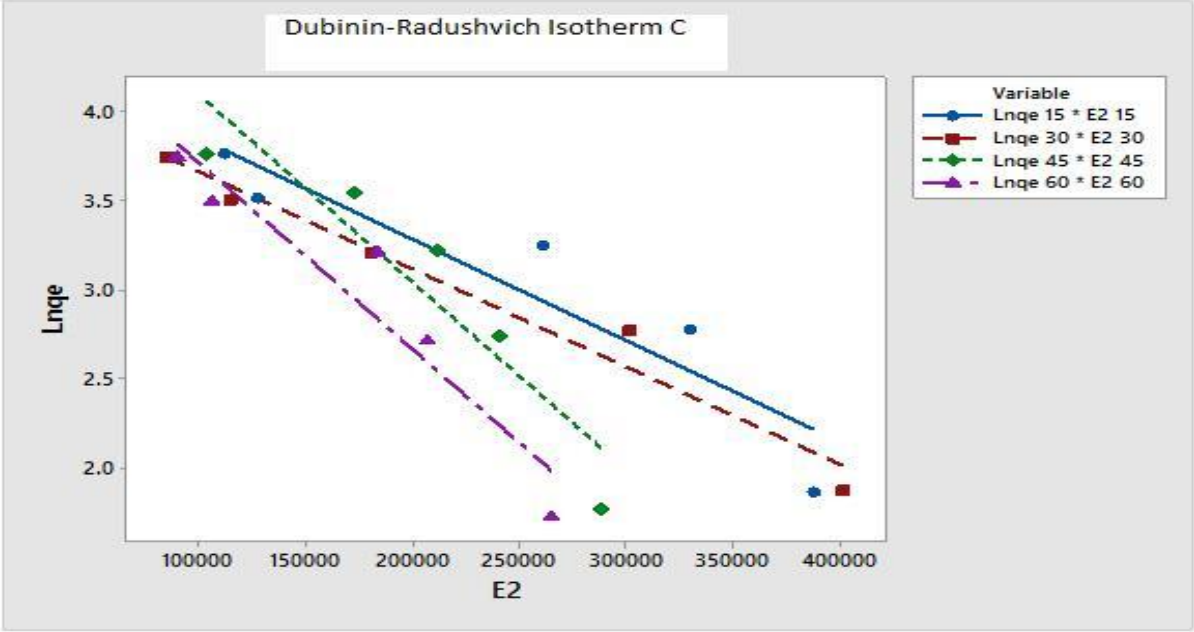

Figure 4. 21: D-R Isotherm Model for Sample C.

From Table 4.8, the free energy (E) was calculated from the value of BD using the formula: $\ln qe = \ln q_D - B_D E^2$. For example, in 5 minutes of shaking time, $\ln qe\ 15 = 3.844 - 0.000002\ E^2$, $r^2 = 0.938$. $\ln q_D = 3.844$, $B_D = 0.000002$ $q_D = e^{3.844}$.

Generally, when the adsorption energy value falls below 8 KJ/kmol, the adsorption process is said to be characterized by physiosorption, implying physical binding of the pesticide to the surface of the soil/sediment. If the value is higher than 8 KJ/mol but less than 20 KJ/mol, it is said to be characterized by ion exchange and similarly, values beginning from 20 KJ/kmol and above are said to be characterized by particle diffusion. From Table 4.8 E (KJ/mol) values were lesser than 8kj/kmol, which implied that the adsorption process of Lamda-Cyhalothrin was

predominantly a physiosorption process. From Figure 4.8 to Figure 4.20, the data fitted well Dubinin-Radushkevich isotherm at the various shaking times for samples A and B whereas sample C has some deviations, yet the coefficient of determination (r^2) ranges from 0.857 to 0.98.

4.4.6 Scatchard Plot Analysis

This analysis provides clear understanding on the affinity of the pesticide to binding sites and to analyze its adsorption result using the following equation:

$$q_e/C_e = Qb - q_e b \ldots\ldots\ldots\ldots\ldots\ldots\ldots\ldots\ldots\ldots\ldots\ldots\ldots (4.2)$$

From Equation (4.12), Q and b become scatchard plot constants when q_e/C_e is plotted against q_e to give a straight line. This means there is one binding site available for adsorption (Homogeneous surface); but when the plots fail to give a straight line then there are more binding sites available for adsorption.

Table 4. 9: Scatchard Analysis Data.

Time (minute)	Sample	bQ_0	B	Q_0	R^2
15	A	5.696	0.01280	445.0000	0.006
	B	4.787	0.03036	157.6745	0.056
	C	1.944	0.1096	17.7372	0.801
30	A	5.526	0.00635	917.4863	0.003
	B	3.280	0.1029	31.8756	0.967
	C	2.006	0.08668	23.1423	0.836
45	A	5.405	0.01197	451.5455	0.006
	B	4.641	0.0534	86.91012	0.196
	C	1.215	0.1301	9.3390	0.889
60	A	4.751	0.03880	122.4485	0.081
	B	4.898	0.0525	97.4726	0.366
	C	1.178	0.1093	10.7777	0.905

From the regression values obtained, only Sample C (Downstream) shows consistence for high adsorption to lambda-Cyhalothrin (0.801, 0.836, 0.889 and 0.905) as seen in Table 4.9.

Figure 4.22 shows the fitting of sediment Sample A (Upstream) adsorption data to Scatchard plot. The data poorly fitted to this plot, the coefficient of determination values (r^2), i.e., 0.006, 0.003, 0.006, and 0.081 are also consistent with these results. The curves are almost parallel in the plain as the ratios of adsorption/desorption are plotted against adsorption as varied Conc. and time in a fixed mass.

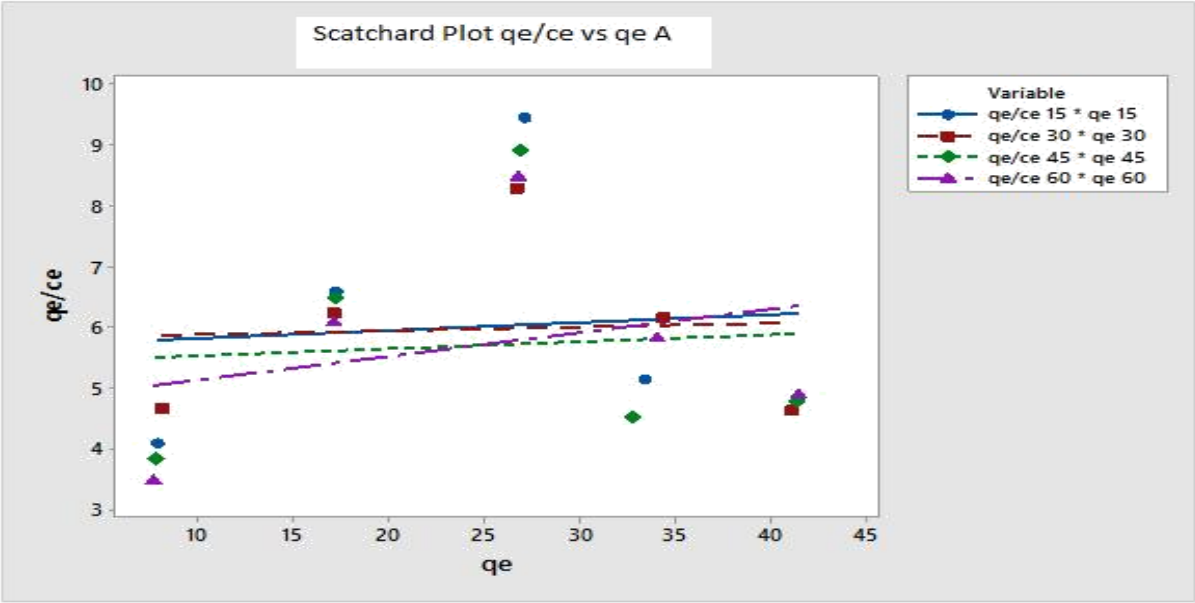

Figure 4. 22: Scatchplot for Sample A.

Figure 4.23 shows the fitting of sediment Sample B (Midstream) adsorption data to Scatchard plot. The data as in Figure 4.22 poorly fitted to this plot. The coefficient of determination values (r^2), i.e., 0.967, 0.056, 0.196, and 0.366 are similar.

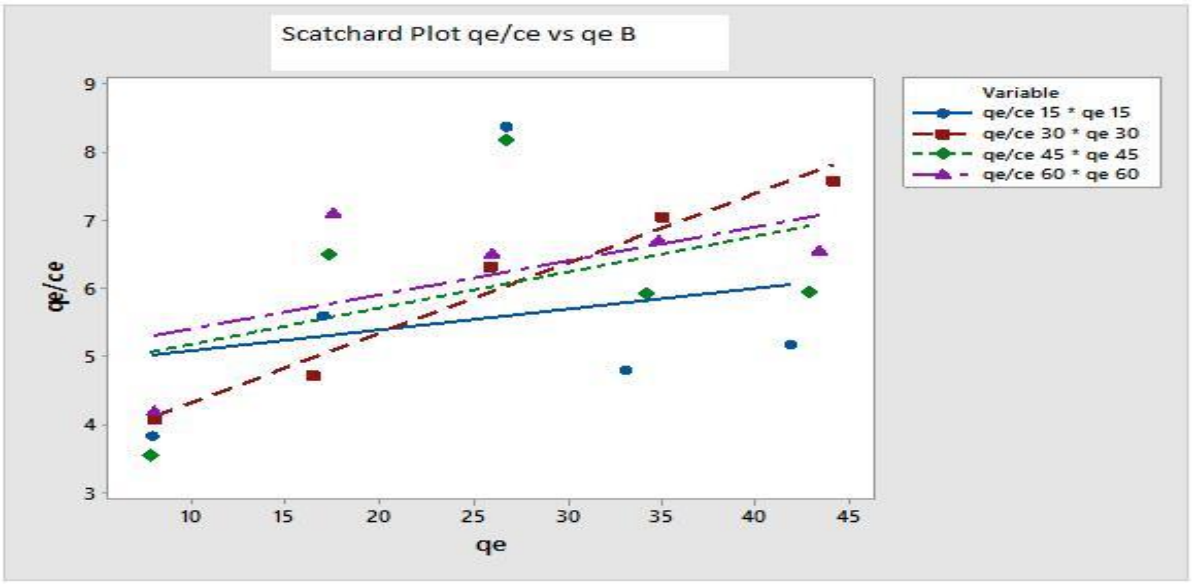

Figure 4. 23: Scatchard Plot for Sample B.

Figure 4.24 shows the fitting of sediment Sample C (Downstream) adsorption data to Scatchard plot. The data fitted well to this plot, the coefficient of determination values (r^2), i.e., 0.801, 0.836, 0.889, and 0.905.

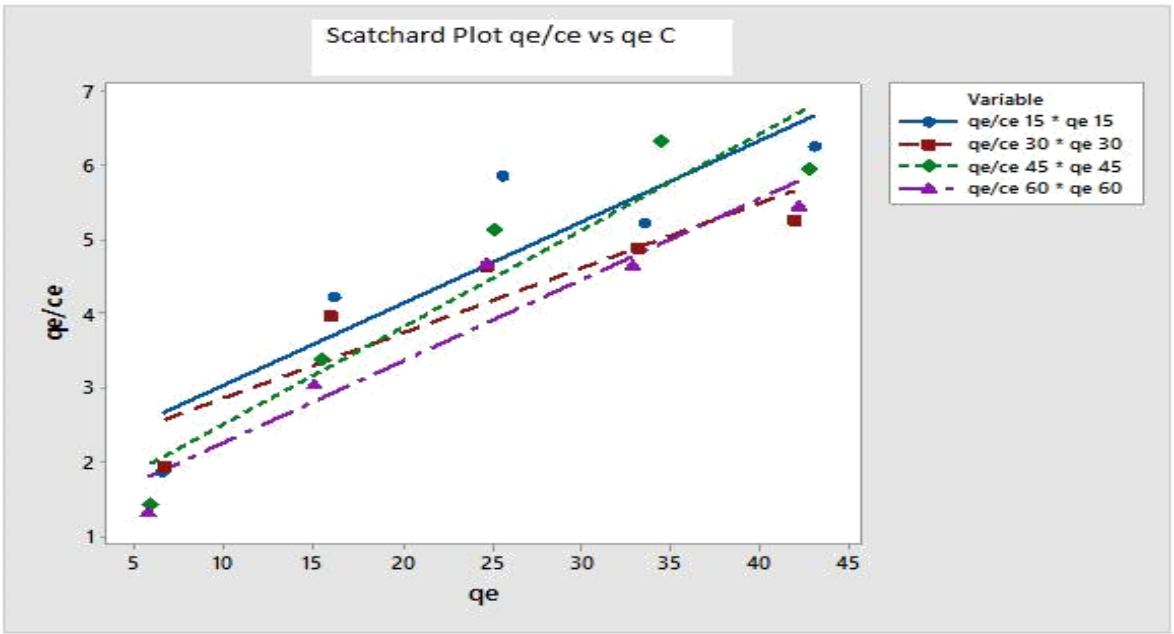

Figure 4. 24: Scatchard Plot for Sample C.

4.5 Degradation Studies

The degradation of pesticides depends on physical, chemical, and biological factors. These include the soil profiles, its organic matter content, the microbial activity in the soil and the acidity of the soil and chemical properties of the pesticides. Chemical factors that influence degradation include hydrolysis, adsorption and desorption.

From the Athi River and Kwale soil profiles (Table 4.2), the soils generally had similar properties. The key ones included medium acidic, low organic matter contents and metallic elements ranging to high. In the overall process, Lambda-Cyhalothrin degraded uniformly in both soils, but the values of degradation were higher in Kwale soil than Athi River soil as seen in Table 4.12. This increased value could be attributed to soil parameters aforementioned.

Table 4.10: Degradation Data for Athi River and Kwale Soils (μg/mL).

SAMPLES	**WK_1** (μg/mL)	**WK_2** (μg/mL)	**WK_3** (μg/mL)	**WK_4** (μg/mL)	**WK_5** (μg/mL)
Athi River Soil	4.40 ±0.42	3.60 ±0.49	3.30 ±0.43	3.00 ±0.22	2.30 ±0.08
Kwale Soil	8.40 ±0.25	7.20 ±1.11	6.50 ±0.65	6.10 ±0.75	4.50 ±0.98

A plot of the amount of L-Cyhalothrin degraded against the number of week gave a non-linear relationship line. This indicates that degradation of the pesticide (Lambda-Cyhalothrin) continued to reduce from week one to the week five.

Figure 4.25 shows the comparative degradation of Lambda Cyhalothrin in Athi River soil and Kwale soil. The trend indicated in the graph shows pattern of degradation in both soils from week one to week five during the experiment, though kwale soil degraded greater amount of L-Cyhalothrin than Athi River soil.

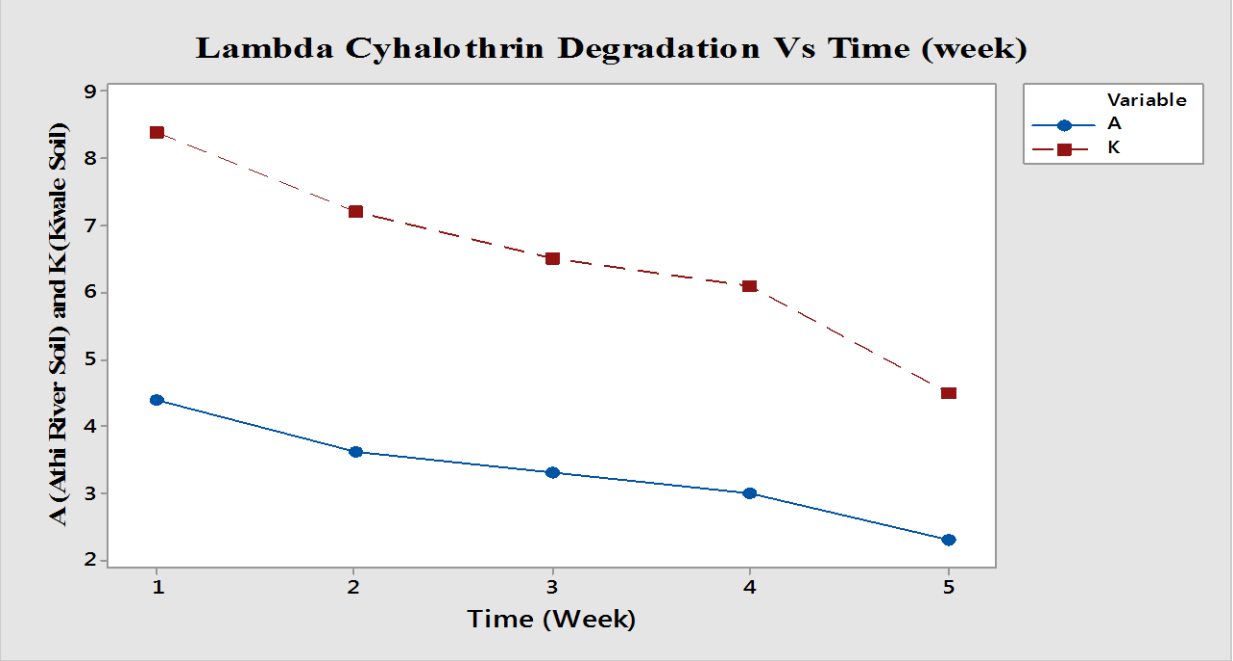

Figure 4. 25: Degradation of L-Cyhalothrin in Athi River and Kwale Soils.

As shown in Figure 4.25, Figure 4.26 is the linearized curve following complete parallel pattern of degradation of L-Cyhalothrin in Athi River soil and Kwale soil.

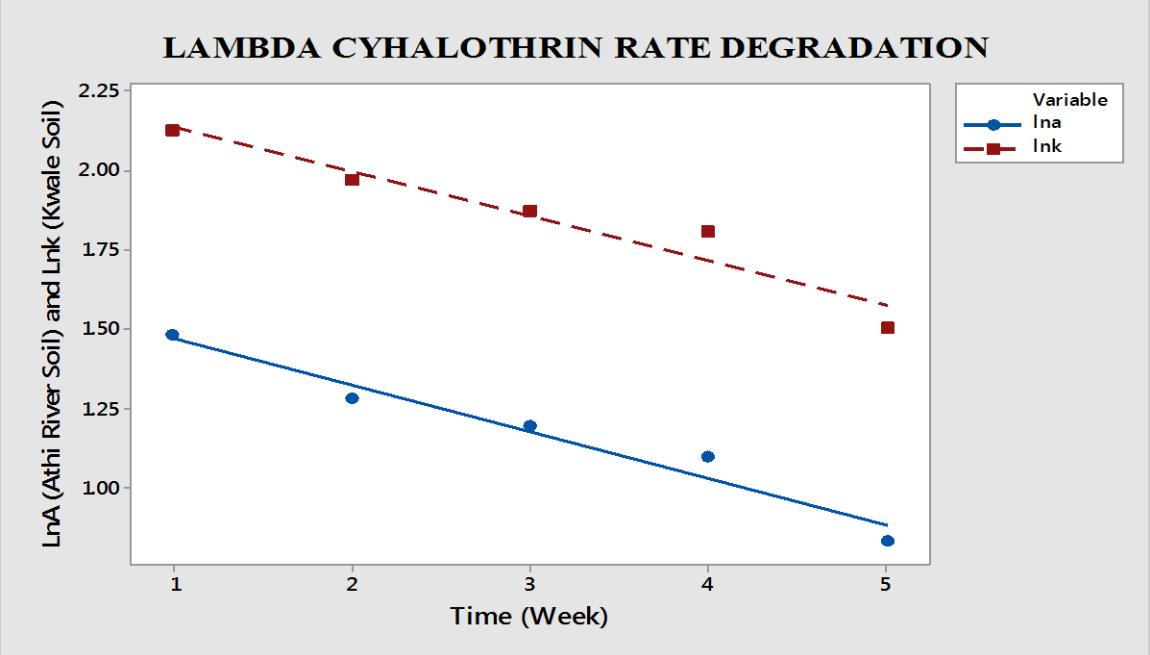

Figure 4. 26: Rate Degradation of L-Cyhalothrin in Athi River and Kwale Soils.

From Figures 4.25 and 4.26, L-Cyhalothrin degraded uniformly in both soil samples, from high to low but at different rates and concentrations. Degradation of Lambda-Cyhalothrin in soils increased with time and was also affected by the soil properties mentioned earlier.

CHAPTER FIVE

5. CONCLUSION AND RECOMMENDATIONS

5.1 Conclusions

1. Adsorption of Lambda-Cyhalothrin decreases with increase in mass of sediment. The longer the contact time the higher the adsorption.
2. Increase in concentration results in decreased percentage (%) adsorption. This is because at high initial concentration the number of moles of Lambda-Cyhalothrin available to the surface area high, so functional adsorption becomes dependent on initial concentration.
3. Adsorption of lambda cyhalothrin followed Freudlich-peterson isotherm model with regression values ranging from 0.954 to 0.992. As shaking time increased from 15 minutes to 60 minutes, the value of n increased from 0.1998 to 0.2914.
4. The value of G was 11.7946 $^{+}$ 0.3Kjol/mol which indicates that adsorption of Lambda-Cyhalothrin by Athi River sediments is spontaneous.

5.2 Recommendation

5.2.1 Recommendation from this Study

Based on the above findings, results and overall discussions of this research project, it is recommended that:

1. The government and agricultural experts should promote use of biological methods of crop pest and diseases control methods to reduce environmental contamination/burden.
2. Environmentalists and scientists should come up with more efficient and effective ways of disposing pesticide residues and residual packaging materials.
3. KEPHIS, KARLO and Pesticide board should come up with Kenyan database containing

pesticide residues in particular area with their mode of safe disposal.

5.2.2 Recommendations for Further Work

Further research work is highly recommended to:

1. Determine the mechanism of pesticide residues degradation in the environment.
2. Determine the amount of lambda cyhalothrin reaching the target area of application to develop more efficient methods of application of pesticides.
3. Further work on adsorption behavior of these residues with respect to change in temperature should be done. This is because of the different weather conditions under which different farmers use these residues.
4. A database should be put in place on how farmers are using different classes of pesticide residues, how they dispose them and more so how they dispose the containers housing these residues.

REFERENCE

Arias, E. M., Lopez, P. E., Simal, G. J., Mejuto, J. C., & Garcia, L. (2008). The mobility and degradation of pesticides in soils and the polluted underground resources. *Agric. Ecosyst. Environ, 123*, 247–260.

Babu, B. R., Meera, K. M. S., & Venkatesan, P. (2011). Removal of pesticide from wastewater by electrochemical methods-a comparative approach. *Sustainable Environmental Research*, *21*, 401–406.

BIS. (1997). *Lambda Cyhalothrin Technical Specification. Bureau of India Standards, Pesticide Sectional Committee, ManakBhavan, 9 Bahadar Shan Zafar Marg*. New Delhi, India.

Bowman, B. T., & Sans, W. W. (1977). Soil Science. *Soc. Am. J.*, *41*, 514–519.

Carroll, D. (1959). Ion Exchange in Clays and other Minerals. *Geological Society of America Bulletin*, *70*(6), 749–780.

Carter, M. R. (1993). Soil Sampling and Methods. CRS Press.

CDPR. (2006). *California Department of Pesticide Regulation. Pesticide Use Database*. California, USA.

CDPR. (2011). California Air Resource Board. Retrieved from cdpr.ca.gov.

De, A. K. (2010). *Environmental Chemistry* (7th ed.) New Delhi: New Age International.

Dubinin, M. M. (1960). The potential theory of adsorption of gases and vapours for adsorbents with energetically non-uniform surfaces. *Chemical Reviews*, *60*(2), 235–241.

Espino, M. P. B. (2008). *Photolytical Degradation Products of Pentachlorophenol in aqueous solution and organic solvents. Philippines Journals of Science*. Institute of Chemistry, College of Science , University of Philippines, Dilima, Queen City, Philippines.

FAO/WHO. (2012). *Evaluation Report based on submission of data from Bhara Rasayan Limited (TC). In: Food and Agriculture Organization. FAO Specifications and evaluations for agricultural pesticides-Lambda Cyhalothrin.* Rome, Italy.

Foo, K. Y., & Hameed, B. H. (2010). Insights into the modelling of adsorption isotherm sytems. *Journal of Chemical Engineering*, *156*, 2–10.

Freundlich, H. M. F. (1906). Over the adsorption in Solution. *Journal of Physical Chemistry*, *57*, 385–471.

Garcia, S. G., Scheilben, D., & Binder, C. R. (2011). The weight method: a new screening method for estimating pesticide deposition from knapsack sprayers in developing countries. *Chemosphere*, *82*, 1571–1577.

Gislason, E. A., & Craig, N. C. (2005). Cementing the Foundations of thermodynamics: comparisons of system-based and surrounding-based definitions of work heat. *The Journal of Chemical Thermodynamics*, *37*(9), 954–966.

GoK. (2003). *Kenya economic recovery strategy for wealth and employment creation 2003-2007. Ministry of Planning and National Development.* Nairobi, Kenya.

He, L. M., Troiano, J., Wang, A., & Kean Goh, K. (2008). *Environmental Chemistry, Ecotoxicity and Fate of Lambda Cyhalothrin*. *Review of Environmental Contamination and Toxicology* (Vol. 195). New York, NY, USA: Springer Cham Heidelberg, New York.

Hem, L., Park, J., & Shim, J. (2010). Residual Analysis of Insecticides (Lambda Cyhalothrin, Luffenuron, Thiamethoxamand Clothianidin) in Pomegranate Using GC-ECD or HPLC-UVD. *Korean Journal of Environmental Agriculture*, *29*(3), 257–265.

Hide, J. M., Kimani, T., & Hide, C. F. (2001). *Informal irrigation in the peri-urban zone of Nairobi, Kenya: an assessment of surface water quality use for irrigation.* Nairobi, Kenya. Retrieved from report od/tn 105 03/03/2001

Hutson, N. D., & Yang, R. T. (2000). Adsorption. *Journal of Colloid and Interface Science*, 189.

Jong, H., & Byoung, J. (1997). Decomposition of Organophosphorus Compounds with Ultraviolet Energy. *Journal of Korean Ind. and Eng. Chemistry*, *9*(1), 28–32.

Kang' ethe, E. K., Ekuttan, C. E., & Kimani, V. N. (2007). Investigation of the prevalence of bovine tuberculosisand risk factors for for human infection with bovine tuberculosis

amongst dairy and non-dairy farming neighbour households in Dangoretti division, Nairobi, Kenya. *East Africa Medical Journal*, *84*(92–95).

Karanja, N., Mutua, G. K., Ayuke, F., Njenga, M., Prain, G., & Kimenju, J. (2010). Dynamics of Soil nematodes and earthworms in urban vegetables irrigated with wastewater in the Nairobi river basin, kenya. *Tropical and Subtropical Agroecosytems*, *12*(3).

Karanja, N., Njenga, M., Prain, G., Kang' ethe, E. K., Kironchi, G., Githuku, C., & Mutua, G. K. (2010). Assessment of environmental and public health hazards in wastewater used for urban agriculture in Nairobi, Kenya. *Tropical and Subtropical Agroecosytems*, *12*.

Kilelu, C. W. (2014). *Wastewater irrigation, farmers' perceptions of health risks and institutional perspectives: a case study in Maila Saba, Nairobi*. Nairobi, Kenya.

Kutto, E. K., Ngigi, M. W., Karanja, N., Kang' ethe, E. K., Berbora, L. C., Lagerkvist, C. J., & Okello, J. (2011). Bacterial Contamination of Kale (Brassica Oleracea acephala) along the supply chain in Nairobi and its environment. *East Africa Medical Journal*, *88*(2), 46–53.

Lagerkvist, C. J., Hess, S., Okello, J., Hansson, H., & Karanja, N. (2013). Food Health risk perceptions among consumers, farmers, and traders of leafy vegetables in Nairobi. *Food Policy*, *38*, 92–104.

Langmuir, I. (1916). The Constitution and Fundamental Properties of solids and Liquids. Part I. solids. *Journal of the American Chemical Society*, *38*(no 11 (1916)), 2221–2295.

Lawler, S. P., Dritz, D. A., Christiansen, J. A., & Comel, A. J. (2007). Effects of Lambda Cyhalothrin on Mosquito Larvae and Predatory Aquatic Insects,. *Pest Management Science*, *63*(3), 234–240.

Lewis, S. E., Brodies, J. E., Bainbridge, Z. T., Rohde, K. W., Davies, A. M., Masters, B. L., & Straftelke, B. (2009). Herbicides: a new threat to the Great Barrier Reef. *Environmental Pollution*, *157*(8), 2470–2484.

Manigandan, G., Nelson, R., & Jeevan, P. (2013). Biogradation of of Lambda Cyhalothrin by Pseudomonas Fluorescens and Trichodermaviridae. *Journal of Microbiology and Biotechnology Research*, *3*(5), 42–47.

Markle, J. C., Van Buuren, B. H., Moran, K. D., & Barefoot, A. C. (2014). Pyrethroid pesticides in municipal wastewater: A baseline survey of publicly owned treatment works facilities in California in 2013. In describing the behaviour and effects of pesticides in urban and agricultural setting. *American Chemical Society*, 177–194.

Mbui, D. (2014). Adsorption of Dursban (Chloropyifos) Pesticides by Loam Soil from Limuru, Kenya: apparent Thermodynamic Properties. *Africa Journal of Physical Sciences*, *1*(1), ISSN: 2313-3317.

McLaughlin, J. (2009). Migration and Health: Implications for development. A case study of Mexican and Jamaican Migrants in Canada's seasonal agricultural wokers program. *Canadian Foundation for the Americas (FOCAL*.

Mehlich, A. (1953). Determination of P, Ca, Mg, K, and NH4. *North Carolina Soil Test Division (Mimeo 1953)*, 23–89.

NPIC. (2015). Lambda Cyhalothrin Technical factsheet. USA. *National Pesticide Information Center*.

Persson, J. A., Marten, W., & O'Halloran, S. (2008). *Handbook for Kjeldahl Digestion*. Denmanrk.

Rajendran, & Phogat, B. S. (2013). Minutes of 342 nd Meeting of Registration Committee Held on 22/09/2013 in Board Room of ASRB, PUSA, New Delhi. *Heranba Industries Limited*.

Serono, D. B., Maravillas, S. L., Ghafari, N., Rivera, C., Quiambao, E., & Lorenzo, M. C. . (2016). Modelling of the Residue Transport of Lambda Cyhalothrin, Cypermithrin, Malathion and Endosulfan in three differnt Environmental Compartments in the Philippines. *Sustainable Environmental Research*. https://doi.org/http://dx.doi.org/10.1016/j.serj.2016.04.010.

Sharda. (2013). *Sharda Lambda Cyhalothrin 1EC Insecticide, Lancaster Pike, suite A, Hockessin, DE 19707*. USA.

Srivastava, V. V., Swamy, M. M., Mall, I. D., Prasad, B., & Mishra, I. M. (2006). Adsorptive removal of phenol by bagasse fly ash and activated carbon: equilibrium, kinetics and thermodynamics. *Colloids Surface*, *A272*, 89–104.

Temkin, M. I., & Pyhev, V. (1940). Kinetics of ammonia synthesis on promoted iron catalysts. *Acta Physicochem.*, *URSS 12*(3), 217–222.

Thompson, G., Swain, J., Kay, & Foster, M. C. F. (2001). The treatment of Pulp and Paper mill effluent: a review. *Bioresource Technology*, *77*, 275–286.

Tuner, R. C., & Clark, J. S. (1966). Lime potential in acid clay and soil suspensions. Trans. Comm. II and IV Int. *Soc. Soil Science*, 208–215.

UNICEF, WHO, NEPAD, DBSA, Micronutrient, I., & GAIN (2005). *Vitamin and Mineral Deficiency, a partnership drive to end hidden hunger in subaharan African*.

Vodrais, E., Fytianos, F., & Bozani, E. (2002). Sorption Description isotherms of Dyes from aqueous solutions and Wastewaters with different sorbent materials. *The International Journal of Global Nest*, *4*(1), 75–83.

Wauchope, R. D., Buttler, T. M., Hornsby, A. G., Augusti, J. N., Beckers, P. W. M., & Burt, J. P. (1992). The SCS/ARS/CES pesticide properties database for environmental decision-making. *Rev. Environ. Contam. Toxicol.*, *123*, 1–155.

Westcot, D. W. (1997). *Quality control of wastewater for irrigation crop production*. Rome, Italy.

WHO (1991). *Strategies for assessing the safety of foods produced by biotechnology: a joint report of FA*.

WHO (2006). *Guidelines for the safe use of wastewater , excreta and grey water: Wastewater use in agriculture.* Geneva.

WHO (2013). Specification and Evaluations for Public Health Pesticides, Lambda Cyhalothrin.

Yang, S. Y., & Chang, W. L. (2005). Use of finite mixture distribution theory to determine the criteria of cadmium concentration in Taiwan farm and soils. *Soil Science*, *170*(no 1(2005)), 55–62.